Plasma properties and atomic processes at medium and high pressures

H. Drawin

Plasma properties and atomic processes at medium and high pressures

H. W. Drawin

Association EURATOM-CEA sur la Fusion, Département de Physique du Plasma et de la Fusion Contrôlée, Centre d'Etudes Nucléaires, B.P. 6, 92260 Fontenay-aux-Roses, France

Résumé. — Quand l'état du plasma s'écarte de l'équilibre thermodynamique local (E.T.L.), les relations d'équilibre ne sont plus valables. Les propriétés thermodynamiques doivent alors être décrites sur la base de modèles dans lesquels les propriétés atomiques individuelles et les réactions élémentaires interviennent. Dans la première partie du texte on donne une description schématique des plasmas soumis à une injection et des pertes d'énergie et qui subissent en plus des contraintes externes sous forme des conditions initiales et de limite. Les équations de bilan pour la densité des particules, la quantité de mouvement et l'énergie de systèmes ouverts sont résumées en incluant des réactions nucléaires. La seconde partie résume les progrès qui ont été faits dans la compréhension des propriétés de quelques types de plasmas en dehors de l'E.T.L. On traite, sur la base des équations de bilan, plus particulièrement la décharge luminescente sous ses différentes formes, les plasmas d'ions négatifs (avec application à la physique des interrupteurs (SF_6) des circuits électriques), la mesure du coefficient collisionnel-radiatif de recombinaison électrons-ions et les plasmas dans les machines du type Tokamak.

Abstract. — When the state of a plasma deviates from local thermodynamic equilibrium (L.T.E.) the equilibrium relations cannot be applied. The thermodynamic properties must then be described on the basis of models in which the individual atomic properties and elementary reactions intervene. The first part of the paper gives a schematic description of a plasma suffering power input, power losses and external constraints in the form of initial and boundary conditions. The rate equations for particle density, momentum and energy of open systems are summarized, including nuclear reactions. The second part gives a review of the progress made in understanding the properties of special types of non-L.T.E. plasmas such as glow discharge plasmas, negative ion plasmas (with application to the physics of SF_6 circuit-breakers) and Tokamak plasmas on the basis of these rate equations.

1. **Introduction.** — We know that an ionised gas enclosed in a box with perfectly reflecting walls at plasma temperature T can at all temperatures T and pressures p thermodynamically be described by the classical equilibrium relations for *ideal* gases (Maxwell-Boltzmann distribution, Planck's law, mass action law in form of the Waage-Guldberg and Saha-Eggert relations, ...). In such a closed system, energy and entropy are state functions, the entropy has a maximum value.

Under real conditions, plasmas are never enclosed in a black-body box with the wall temperature equal to the plasma temperature T. They rather show more or less strong temperature and density gradients leading to particle, momentum, energy and entropy fluxes between different spatial regions. Photons have the largest mean free path and therefore transport momentum, energy and entropy over much larger distances than material particles. Very often the reabsorption in laboratory plasmas is so weak that most of the photon energy can freely escape. Thermodynamically speaking, under actual conditions plasmas represent *open system* which are generally far from *complete thermodynamic equilibrium* and which may even be far from *local thermodynamic equilibrium* (L.T.E.). Plasmas not obeying the classical thermodynamic equilibrium relations are termed *non-L.T.E. plasmas*.

From a general point of view, a realistic model for a non-L.T.E. plasma, which applies to both laboratory and astrophysical situations, is shown in figure 1. In order to maintain some spatial region S in an ionised state, energy must be fed into S. This energy may come from an external source (e.g. the electrical power supply G, a photon ($h\nu_+$) or particle (p) flux) or it may be produced by the plasma itself (chemical or nuclear reactions). In the most general case we have also to admit electric ($\mathfrak{E}$) and magnetic ($\mathbf{B}$) fields. The *stationary state* in mechanical equilibrium is characterized by a *dynamic equilibrium* between all particle, momentum and energy fluxes. For instance, the ambipolar diffusion flux must be compensated by an equivalent neutral particle flux in opposite direction in order to obtain a stationary density distribution.

In the *non-stationary state* these quantities show a transient behavior. In both cases boundary conditions have an important influence on the plasma state. The external electric components (R, L, G) which close the electric current loop are part of the electrical boundary conditions (which may be time-dependent); but under special (especially astrophysical) conditions they appear sometimes not to be well-separated from the plasma proper which is investigated.

This paper reviews some aspects of the progress

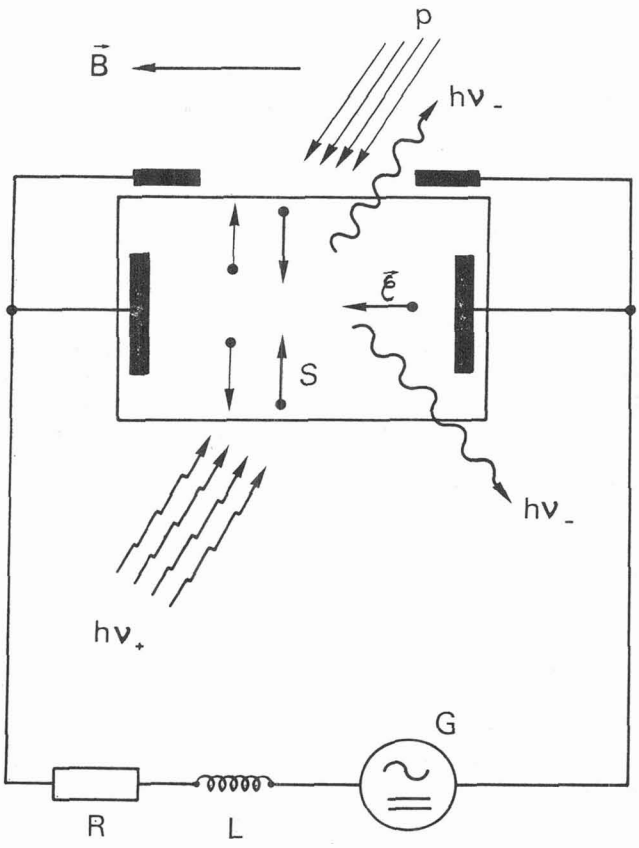

Fig. 1. — Schematic representation of a plasma suffering power input, power losses and constraints in the form of initial and boundary conditions. For further details see text.

made during the last years in describing non-equilibrium effects in laboratory plasmas at medium and high pressures. The terms *medium* and *high* pressures should in the present context only be considered as an indication that practically at all pressures of interest atomic processes in the widest sense are necessary in order to describe the plasma properties under non-L.T.E. conditions. These processes are essential when one wants to understand how a system evolves towards equilibrium. *Non-ideal* plasmas will not be treated here. (Concerning the definition and general properties of non-ideal plasmas the reader is referred to [1-4].) Also wave phenomena such as ionisation and chemical waves will be excluded from our considerations.

2. **The basic equations.** — Before discussing particular experimental situations and results it might be useful to summarize the basic equations by which plasmas can consistently be described. We shall adopt a more general point of view as is usually done, in agreement with the introductory remark that plasmas represent open systems, i.e. that they exchange particles, momentum and energy with the external world. Our starting point is the kinetic collision (Boltzmann) equation

$$\frac{\partial f_s}{\partial t} + \sum_{\beta=1}^{\beta=3} w_\beta \frac{\partial f_s}{\partial x_\beta} + \sum_{\beta=1}^{\beta=3} \frac{I_{s,\beta}}{m_s} \frac{\partial f_s}{\partial w_\beta} = \left[\frac{\partial f_s}{\partial t}\right]_{\substack{\text{collisin} \\ \text{radiation}}} \tag{1}$$

and its various velocity moments. $f_s(\mathbf{r}, \mathbf{w}, t)$ is the velocity distribution function of particles of species $s = s(z, k, i)$ as a function of space point $\mathbf{r}$, velocity $\mathbf{w}$ in the laboratory system and time t. $\beta = 1, 2, 3$ represents the three coordinate directions. m_s is the particle mass and $F_{s,\beta}$ represents the (external) forces $\mathbf{F}$ exerted on s in the direction β (e.g. due to electric or magnetic fields). s stands for electrons or z-times ionised chemical species k in quantum state $|\, i \,\rangle$. The right-hand side of eq. (1) is the rate of change of f_s due to collision and radiation processes. Integration of f_s over $\mathbf{w}$ yields the particle density of species s :

$$\iiint f_s(\mathbf{r}, \mathbf{w}, t)\, \mathrm{d}w_1\, \mathrm{d}w_2\, \mathrm{d}w_3 = n_r(\mathbf{r}, t)\,. \tag{2}$$

Instead of $\mathbf{w}$ we can consider f_s as a function of the momentum $m_s w = \mathbf{p}$ of a particle : $f_s = f_s(\mathbf{r}, \mathbf{p}, t)$. The eq. (1) can then also be written as

$$\frac{\partial f_s}{\partial t} + \mathbf{w}_s . \nabla_r f_s + \mathbf{F}_s . \nabla_p f_s = \left[\frac{\partial f_s}{\partial t}\right]_{\substack{\text{coll.} \\ \text{rad.}}} \tag{3}$$

In this form the kinetic collision equation is also applicable to photons (massless particles) : the velocity and momentum of a photon of frequency ν traveling in the direction of unit vector $\mathbf{u}$ are (c is the velocity of light, h is Planck's constant) :

$$\mathbf{w}_s = \mathbf{w}_\nu = \mathbf{u}c \tag{4}$$

$$\mathbf{p}_s = \mathbf{p}_\nu = \mathbf{u}h\nu/c\,. \tag{5}$$

For photons, $\mathbf{F}_s = \mathbf{F}_\nu$ is in nearly all cases negligible. Thus, eq. (3) reduces to

$$\frac{\partial f_\nu(\mathbf{u})}{\partial t} + c\mathbf{u} . \nabla_r f_\nu(\mathbf{u}) = \left[\frac{\partial f_\nu(\mathbf{u})}{\partial t}\right]_{\substack{\text{coll.} \\ \text{rad.}}} \tag{6}$$

which represents the time-dependent radiative transport equation. $f_\nu(\mathbf{u})\, \mathrm{d}\nu$ is the number of photons with frequencies between ν and $\nu + \mathrm{d}\nu$ traveling in the direction $\mathbf{u}$. The specific intensity $I_\nu(\mathbf{u})$ and $f_\nu(\mathbf{u})$ are linked through the relation

$$I_\nu(\mathbf{u})\, \mathrm{d}\nu = \frac{2h\nu^3}{c^2} f_\nu(\mathbf{u})\, \mathrm{d}\nu\,. \tag{7}$$

Integrating eq. (1) or eq. (3) over $\mathbf{w}$ yields the rate equation for the macroscopic quantity $n_s(\mathbf{r}, t)$:

$$\frac{\partial n_s}{\partial t} + \nabla_r . (n_s \langle \mathbf{w}_s \rangle) = \left[\frac{\partial n_s}{\partial t}\right]_{\substack{\text{coll.} \\ \text{rad.}}} \tag{8}$$

where $\langle \mathbf{w}_s \rangle$ is the mean species velocity in the laboratory system. We introduce the mean mass velocity $\mathbf{v}_0$ of the plasma as a whole and the species peculiar ($\mathbf{V}_s$) and mean diffusion velocity ($\langle \mathbf{V}_s \rangle$) by

$$\mathbf{w}_s = \mathbf{v}_0 + \mathbf{V}_s ; \qquad \langle \mathbf{w}_s \rangle = \mathbf{v}_0 + \langle \mathbf{V}_s \rangle . \quad (9)$$

In a coordinate system at rest with respect to the total plasma motion of velocity $\mathbf{v}_0$ we thus have

$$\frac{\partial n_s}{\partial t} + \nabla_r . (n_s \langle \mathbf{V}_s \rangle) = \left[\frac{\partial n_s}{\partial t}\right]_{\substack{\text{coll.} \\ \text{rad.}}} \quad (10)$$

$n_s \langle \mathbf{V}_s \rangle$ can be expressed by the phenomenological relation ($q_s = e_0 z_s$ is the species electric charge)

$$\mathbf{j}_s = q_s n_s \langle \mathbf{V}_s \rangle = - \boldsymbol{\sigma}_s^{dc} : \mathbf{E}^0 - \boldsymbol{\sigma}_s^{ac} : \tilde{E} - q_s \mathbf{D}_s : \nabla_r n_s - q_s \boldsymbol{\theta}_s : \nabla_r T \quad (11)$$

where $\mathbf{E}^0$ and $\mathbf{E}$ are the *dc* and *ac* electric fields. Further $\boldsymbol{\sigma}^{dc}$ and $\boldsymbol{\sigma}^{ac}$ are the corresponding electrical conductivities, $\mathbf{D}_s$ and $\boldsymbol{\theta}_s$ represent the particle diffusion and thermal diffusion coefficients respectively. In the most general case they represent tensors. Eq. (10) is the diffusion equation and will be discussed in connection with the glow discharge problem. The crucial point is to express the right-hand side and $\langle \mathbf{V}_s \rangle$ as a function of the atomic and nuclear reaction processes.

Summation over s of all eq. (10) yields the following rate equation for the total particle density $n = \sum n_s$:

$$\frac{\partial n}{\partial t} + {}_s\sum \nabla_r . (n_s \langle \mathbf{V}_s \rangle) = \left[\frac{\partial n}{\partial t}\right]_{\substack{\text{coll.} \\ \text{rad.}}} \quad (12)$$

The right-hand side is not necessarily zero. For an isolated system one has

$$\left[\frac{\partial n}{\partial t}\right]_{\substack{\text{coll.} \\ \text{rad.}}} = \left[\frac{\partial n_e}{\partial t}\right]_{\substack{\text{coll.} \\ \text{rad.}}} + \left[\frac{\partial n_M}{\partial t}\right]_{\substack{\text{coll.} \\ \text{rad.}}} + \left[\frac{\partial n_{\text{nucl}}}{\partial t}\right]_{\substack{\text{coll.} \\ \text{rad.}}} \quad (13)$$

where the first term on the *r-h-s* accounts for the creation and destruction of electrons due to collisional-radiative processes, the second one takes into account the collisional-radiative formation and destruction of molecules, and the last one nuclear transformations (e.g. D + T → He + n, see eq. (86)). Only in completely dissociated and ionised gases will the first two terms be zero.

The form of eq. (12) is sufficiently general to include open systems, i.e. where a plasma is submitted to a beam of particles or photons. Also nuclear reactions can be taken into account by the term on the right-hand side.

The rate equation for the total mass density $\rho = \sum n_s m_s$ is given by

$$\frac{\partial \rho}{\partial t} + \nabla_r . (\rho \mathbf{v}_0) = \left[\frac{\partial \rho}{\partial t}\right]_{\substack{\text{coll.} \\ \text{rad.}}} \quad (14)$$

For an isolated system, the right-hand side is zero, since collisions alone cannot change the total density. Eq. (13) has then the form of a conservation equation. When the plasma is submitted to a stream of particles (e.g. neutral particle injection) or when nuclear reactions take place the right-hand side is different from zero (e.g. in reaction (86) one loses the neutron and mass which is transformed into kinetic energy).

Multiplication of eq. (1) by $m_s \mathbf{w}$ or $m_s \mathbf{ww}$ and integration over $\mathbf{w}$ yields respectively the rate equations for the momentum density and the pressure tensor $\mathbf{P}_s = n_s m_s \langle \mathbf{w}_s \mathbf{w}_s \rangle$ of species s. The equation for the momentum density is :

$$\frac{\partial}{\partial t}(n_s m_s \langle \mathbf{w}_s \rangle) + \nabla_r . (n_s m_s \langle \mathbf{w}_s \mathbf{w}_s \rangle) - n_s \mathbf{F}_s = \left[\frac{\partial}{\partial t} n_s m_s \langle \mathbf{w}_s \rangle\right]_{\substack{\text{coll.} \\ \text{rad.}}} \quad (15)$$

Summing over all species s and substituting $\mathbf{w}_s$ by eq. (9) yields the rate equation for the momentum density for the whole plasma as a function of $\mathbf{v}_0$. Taking eq. (8) into account finally yields

$$\frac{\partial \mathbf{v}_0}{\partial t} + \mathbf{v}_0 . \nabla_r \mathbf{v}_0 + \frac{1}{\rho} \nabla . \mathbf{P} - \frac{1}{\rho} {}_s\sum n_s \mathbf{F}_s = \left[\frac{\partial \mathbf{v}_0}{\partial t}\right]_{\substack{\text{coll.} \\ \text{rad.}}} \quad (16)$$

where $\mathbf{P} = {}_s\sum \mathbf{P}_s$ is the total pressure tensor. The right-hand side is generally zero, since collisions between plasma particles alone cannot change $\mathbf{v}_0$. Under special conditions however, it can be different from zero. This is for instance the case when a plasma is submitted to a spatially anisotropic beam of energetic particles or photons. (The observed rotation of a Tokamak plasma when it is submitted to tangential neutral particle injection belongs to such a case.) When the right-hand side of eq. (16) is put equal to zero, a corresponding contribution must formally be taken into account on the left-hand side.

The rate equation for the pressure tensor is

$$\frac{\partial}{\partial t}(n_s m_s \langle \mathbf{w}_s \mathbf{w}_s \rangle) + \nabla_r . (n_s m_s \langle \mathbf{w}_s \mathbf{w}_s \mathbf{w}_s \rangle) - 2 n_s \mathbf{F}_s \langle \mathbf{w}_s \rangle = \left[\frac{\partial}{\partial t} n_s m_s \langle \mathbf{w}_s \mathbf{w}_s \rangle\right]_{\substack{\text{coll.} \\ \text{rad.}}} \quad (17)$$

Dividing this equation by two and taking the trace yields the rate equation for the kinetic energy density $(1/2)\, n_s m_s \langle w_s^2 \rangle$. Eq. (17) does not contain the internal energy (excitation, dissociation, ionisation energies). The rate equation for the internal energy density of species s is

$$\frac{\partial n_s E_s^{\text{int}}}{\partial t} + \mathbf{v}_r . (n_s E_s^{\text{int}} \langle \mathbf{w}_s \rangle) = \left[\frac{\partial n_s E_s^{\text{int}}}{\partial t}\right]_{\substack{\text{coll.} \\ \text{rad.}}} \quad (18)$$

E_s^{int} is the internal energy per particle of species s.

Summing up the eqs. (17) and (18) over all s yields the rate equation for the energy density of the plasma as a whole. One can now express all collisional-radiative terms as a function of rate coefficients and particle densities. When one takes still into account the eqs. (9) and (12) one finally obtains the following rate equation for the thermal plus internal energy density

$$\frac{\partial}{\partial t}(U^{\text{th}} + U^{\text{int}}) + \nabla.(U^{\text{th}} + U^{\text{int}})\,\mathbf{v}_0 + \\ + U^{\text{th}}\,\nabla.\mathbf{v}_0 + \nabla.\mathbf{Q}^{\text{total}} + \dot{R} = \dot{\Omega} + \dot{I} + \dot{N} \quad (19)$$

where

$U^{\text{th}} = \frac{3}{2} n_{\text{h}} kT_{\text{h}} + \frac{3}{2} n_e kT_e$ (total thermal energy density),

$U^{\text{int}} = \sum n_s E_s^{\text{int}}$ (total internal energy density),

$\mathbf{Q}^{\text{total}} = \mathbf{Q}^{\text{th}} + \mathbf{Q}^{\text{int}}$ (total heat flux vector),

$\dot{\Omega}$ = ohmic (electric) power input,
$\dot{I}$ = power input by particle injection,
$\dot{N}$ = nuclear power heating rate,
$\dot{R}$ = radiative loss rate.

$\dot{R}$ contains contributions from free-free (*f-f*), free-bound (*f-b*), bound-bound (*b-b*), dielectronic (*di*) and cyclotron (*c*) radiation :

$$\dot{R} = \dot{R}^{ff} + \dot{R}^{fb} + \dot{R}^{bb} + \dot{R}^{\text{di}} + \dot{R}^{c}. \quad (20)$$

It should be mentioned that the radiative transfer eq. (6) intervenes in the calculation of $\dot{R}$ and that $\dot{\Omega}$, $\dot{I}$ and $\dot{N}$ contain contributions which are different for the electrons (*e*) and heavy particles (*h*). For instance, the 3.5 MeV α-particles created in a thermonuclear D-T plasma will preferentially heat the electrons. The ions will directly gain energy from the α-particles when most of their energy has been slown down already. Details of this slowing-down process are described by eq. (1) in form of the Fokker-Planck equation.

The eqs. (19)-(20) will be discussed in connection with the energy loss of Tokamak plasmas.

In order to describe a plasma completely one has still to add the Maxwell equations, the charge neutrality condition and the initial and boundary conditions.

In the following we will successively treat the glow discharge plasma in molecular and atomic gases, the so-called constriction phenomenon, the recombination of SF_6 plasmas in electric circuit breakers and the problem of measuring collisional-radiative recombination coefficients in general, the dynamics of hydrogen, helium, oxygen and the problem of radiation losses in Tokamak plasmas. The latter ones must already now be considered as *high-pressure* plasmas although their density is still relatively low. Fast transient phenomena as they are encountered in laser beam-plasma interaction will only be discussed in connection with the determination of rate coefficients from laser beam-induced fluorescence measurements of a stationary plasma.

3. **The glow discharge plasma.** — The plasma of a glow discharge is very far from L.T.E. Although the macroscopic properties such as the dependence of the mean electron temperature T_e and mean electron density n_e on the gas pressure p, and the dependence of the electric field strength $\mathcal{E}$ on the electric current I are in principal well known, finer details of these dependences related to atomic and molecular processes have still to be discovered. Especially a number of atomic and molecular processes in these discharges and their influence on the thermodynamic properties and the space-dependent values of T_e, n_e and I are still not well understood. In particular, one has not yet a satisfactory explanation of the so-called constriction phenomenon.

3.1 THE GLOW DISCHARGE ; BASIC CONSIDERATIONS. — To begin with, let us briefly recall the basic theoretical assumptions and results for the positive column of a glow discharge (for the details see [5-8]) in the frame of the Schottky theory :

— the plasma is quasi-neutral, i.e. $n_e \cong n_+$, $|n_+ - n_e| \ll n_e$;
— the electron temperature T_e is constant across the discharge;
— the electron velocity distribution is maxwellian;
— the electron mobility is given by Langevin's equation;
— the ion-electron production rate is proportional to n_e;
— the gas temperature is constant across the discharge and can be considered as a given quantity.

Simple considerations about the particle and energy balance lead to relations for T_e, the electron density n_e and the electric strength $\mathcal{E}$ as a function of given external parameters such as gas pressure p, radius R of the discharge tube, the electric (or plasma) current I and the kind of gas employed.

The balance equations for the electron and ion densities, n_e and n_+, are (see eq. (10)) :

$$\frac{\partial n_e}{\partial t} + \nabla_r.(n_e \langle \mathbf{V}_e \rangle) = \left[\frac{\partial n_e}{\partial t}\right]_{\substack{\text{coll.}\\ \text{rad.}}} \quad (21a)$$

$$\frac{\partial n_+}{\partial t} + \nabla_r.(n_+ \langle \mathbf{V}_+ \rangle) = \left[\frac{\partial n_+}{\partial t}\right]_{\substack{\text{coll.}\\ \text{rad.}}} \quad (21b)$$

where the right-hand sides represent the collisional-radiative source terms (sum of ionisation and recombination rates). $\langle \mathbf{V}_e \rangle$ and $\langle \mathbf{V}_+ \rangle$ are the mean diffusion velocities of electrons and ions respectively. For a cylindrical plasma column, a radial electric fields is build up due to the radially diffusing electrons and ions. This field causes the electron-ion pairs to

diffuse with the same radial ambipolar diffusion velocity. The diffusion flux is described by :

$$[n_e \langle \mathbf{V}_e \rangle]_r = [n_+ \langle \mathbf{V}_+ \rangle]_r = - D_a \nabla_r n_e = - D_a \nabla_r n_+ \quad (22)$$

where D_a is the ambipolar diffusion coefficient. Further, the right-hand sides of eqs. (21*a*), (21*b*) are equal because of charge neutrality. One makes now the assumption that the collisional-radiative source term is proportional to n_e :

$$\left[\frac{\partial n_e}{\partial t}\right]_{\substack{\text{coll.}\\ \text{rad.}}} = \left[\frac{\partial n_+}{\partial t}\right]_{\substack{\text{coll.}\\ \text{rad.}}} = n_e n_0 S \quad (23)$$

where $S = \langle \sigma_1 v \rangle$ is the ionisation coefficient for electron-neutral atom (molecule) collisions. Owing to the eqs. (22)-(23), the eqs. (21*a*), (21*b*) can be replaced by one single equation :

$$\frac{\partial n_e}{\partial t} - D_a \nabla^2 n_e = n_0 n_e S . \quad (24)$$

For a stationary cylindrical plasma column one obtains the equation :

$$D_a \frac{1}{r} \frac{\partial}{\partial r}\left(r \frac{\partial n_e}{\partial r}\right) + n_0 n_e S = 0 . \quad (25)$$

Since S is assumed to be independent of n_e (which implicitely means that volume recombination is omitted), the solution of eq. (25) is for the fundamental mode

$$n_e(r) = n_e(0) J_0\left(r \sqrt{\frac{n_0 S}{D_a}}\right) \quad (26)$$

where $n_e(0)$ is the density at the axis ($r = 0$). For $r(n_0 S/D_a)^{1/2} = 2.405$ the Bessel function is zero, $J_0 = 0$, and for larger values of $(n_0 S/D_a)^{1/2}$ one would get negative values. This would have no physical meaning. Thus, by assuming that the electron density is practically zero at the wall at $r = R$, one imposes the boundary condition :

$$R\left[\frac{n_0 S}{D_a}\right]^{1/2} = 2.405 \quad (27)$$

and obtains the following radial density distribution :

$$n_r = n_r(0) J_0\left(2.405 \frac{r}{R}\right) . \quad (28)$$

The boundary condition (27) leads to the *similarity law* for the electron temperature T_e in the following way : S is only a function of T_e and the kind of gas via the ionisation cross-section ; hence :

$$S = S(T_e, \text{kind of gas}) . \quad (29)$$

Further, D_a can be expressed in terms of the individual ion diffusion coefficient D_i (see e.g. p. 143 of [8] or pp. 261-262 of [9])

$$D_a = D_i\left(1 + \frac{T_e}{T_0}\right) \quad (30)$$

where T_0 is the gas temperature (assumed to be equal to the ion temperature T_+). For D_i we can now apply the formula for the binary ion (+)-neutral (0) diffusion coefficient (see e.g. pp. 484-486, pp. 523-527 of [10], p. 345 of [11]) as given by the transport theory :

$$D_i = \frac{3}{16} \frac{1}{(n_+ + n_0) \langle \sigma \rangle_{+0}} \left[\frac{2 \pi k T_0}{\mu}\right]^{1/2} \quad (31)$$

where $\langle \sigma \rangle_{+0}$ is some average effective momentum transfer cross-section and μ the reduced mass. Since $n_+ \ll n_0$ and $m_+ = m_0$ (and thus $\mu = m_0/2$) we have :

$$D_a = \frac{3}{8} \frac{1}{n_0 \langle \sigma \rangle_{+0}} \left[\frac{\pi k T_0}{m_0}\right]^{1/2} \left(1 + \frac{T_e}{T_0}\right) = \frac{1}{n_0} F_a(T_e, T_0, \text{kind of gas}) \quad (32)$$

where F_a depends only on T_e, T_0 and on the nature of the gas through the cross section $\langle \sigma \rangle_{+0}$ for ion-neutral collisions. Substituting in eq. (27) S and D_a by the relations (29) and (32) respectively and expressing n_0 by the gas pressure $p = n_0 k T_0$ yields the following similarity law for the electron temperature of the positive column of the glow discharge :

$$R^2 p^2 = F_1(T_e, T_0, \text{kind of gas}) \quad (33)$$

where F_1 is a function which still depends on the nature of the gas through the electronic ionisation and the ion-neutral momentum transfer cross-sections. Since one does generally not know what type of collisions (elastic ion-neutral, charge exchange, excitation transfer, ... collisions) really contribute to $\langle \sigma \rangle_{+0}$ in which proportions, one often expresses D_a in eq. (32) in terms of independently measured ion mobilities. An *analytical* expression for T_e is obtained when a suitable energy dependence of σ_1 is assumed. One generally takes the linear dependence

$$\sigma_1 = a_1(E - E_1)$$

where E_1 is the ionisation energy and a_1 a gas-dependent constant.

In the same manner one can obtain similarity laws for the electric field strength $\mathcal{E}$ and the electron density $n_e(0)$ on the axis [5-8] :

$$\frac{\mathcal{E}}{p} = F_2(p.R, T_0, \text{kind of gas}) \quad (34)$$

$$R^2 n_e(0) = IF_3(p, R, T_0, \text{kind of gas}) \quad (35)$$

where the functions F_2 and F_3 depend on the nature of the gas through elastic and inelastic cross-sections for collisions between electrons and neutrals and on the ion-neutral momentum transfer cross-sections.

I have treated the Schottky theory of the collision-dominated glow discharge plasma in some length in order to show how many assumptions intervene in the derivation of the similarity laws and how they depend on the atomic cross-sections. It is evident that for instance the calculation of T_e can be erroneous in the case of gas mixtures containing constituents of very different ionisation energies and very different cross-sections for ion-neutral collisions which contribute to the effective $\langle \sigma \rangle_{+0}$. A classical example is the helium discharge with small admixtures of neon. The latter increase the axial field strength compared to the pure helium discharge [12]. Dote and Kaneda [13] observed by means of a double probe that also T_e increases. The effect is explained as being due to resonance excitation of neon by helium metastable atoms. This shows that still other atomic processes than those contained in the simple Schottky theory intervene and that the omittance of both stepwise excitation followed by ionisation and volume recombination may represent a severe limitation to the applicability of the theory. Also radiative emission and absorption processes have to be taken into account. The influence of the ensemble of all collision and radiation processes on the electron production rate can be expressed in terms of the collisional-radiative coefficients for ionisation S and recombination α which both depend on T_e and n_e in the simplest case. Replacing in eq. (23) the collisional-radiative source term by the expression

$$\left[\frac{\partial n_e}{\partial t}\right]_{\substack{\text{coll.}\\ \text{rad.}}} = \left[\frac{\partial n_+}{\partial t}\right]_{\substack{\text{coll.}\\ \text{rad.}}} = n_e[n_0\, S(n_e, T_e) - n_+\, \alpha(n_e, T_e)] \quad (36)$$

leads to a non linear boundary-value problem which permits a formal analytic solution [14-16], see also [34].

In eqs. (24) (36), the function S — and thus F_1, F_2 and F_3 — depends strongly on the exact form of the velocity distribution function $f(E)$ of the electrons which, in turn, depends in a complicated manner on all elastic, inelastic, superelastic and radiative processes. In order to avoid the calculation of $f(E)$ one sometimes replaces the Maxwell distribution by a Druyvesteyn distribution. The latter is obtained from the electron energy balance equation when one assumes that the energy which an electron gains in the electric field is only lost through elastic collisions. However, when inelastic collisions (excitation, ionisation) are added to the energy balance equation, the Druyvesteyn dependence $f(E) \propto E^{1/2} \exp(-0.55(E/\bar{E})^2)$ changes into a modified Maxwell distribution

$$f(E) \propto E^{1/2} \exp(-E/\bar{E}) .$$

(For the details see e.g. pp. 548-550 of [6].) For the same mean translational energy $\bar{E}$ the two distributions give for the reaction coefficients values which can differ by several orders of magnitude. Under real conditions, $f(E)$ has a complicated E — dependence which lies in general somewhere between a $E^{1/2} \exp(-(E/\bar{E})^2)$ and $E^{1/2} \exp(-E/\bar{E})$ dependence. The determination of the mean translational energy $\bar{E}$ (i.e. of kT_e) of the electron gas by means of the similarity law can therefore only give an approximate value, it is not a precise method.

In most papers $f(E)$ is now directly calculated from eq. (1). The energy dependence of such calculated distribution functions depends on the individual processes and their cross-sections. It should be mentioned that most of the published results are inconsistent from the thermodynamic point of view (although they often reproduce the experimental results quite well), since they do not account for superelastic collisions. It might be that inclusion of these processes in the model together with diffusion of excited species will bring experimental and theoretical results in better agreement. It should be emphasized that the superelastic collisions play a dominant role during the recombination phase and in situations where strong resonance absorption leads to high overpopulation of the first resonance levels.

Due to the non thermal population of excited atomic (ionic) levels it is difficult to obtain reliable experimental T_e-values from the *Boltzmann ratio*. In general they are too low. A better method is to determine T_e from a measurement of a number of spectral line intensities without using individual Boltzmann ratios. This method applied in [17-18] to a diffusion-dominated plasma column makes use of the solutions for the excited state populations of an appropriate collisional-radiative model and their comparison with spectroscopically determined population densities. It gives reliable values provided the atomic quantities (such as transition probabilities, cross-sections, line broadening parameters, ...) are known.

Already for the obviously simplest case, namely a glow discharge plasma in hydrogen gas, many of the relevant cross-sections for collisions between hydrogen atoms and hydrogen molecules are still unknown. Therefore a sophisticated model which makes use of the collisional-radiative model will not give more reliable values than the simple Schottky theory as long as all collision processes are not well understood. New results, which have led to a better understanding of the physical processes in a glow discharge plasma in molecular gases, were recently obtained by Dubreuil and Catherinot [19] who studied the reaction kinetics of excited hydrogen atoms and excited hydrogen molecules. Since their paper touches a general aspect common to all molecular plasmas, it shall be discussed in some detail.

3.2 THE GLOW DISCHARGE IN HYDROGEN GAS. — Dubreuil and Catherinot [19] studied the emission

of both the atomic and molecular species of hydrogen by means of laser-induced fluorescence. The discharge capillary had a diameter of $2R = 4$ mm, current and pressure were varied between the following values :

$$5 \leqslant I(\text{mA}) \leqslant 40 ;$$

$$0.1 \leqslant p(\text{torr}) \leqslant 2 .$$

For each value of I and p the mean electron density n_e was determined from the frequency shift of the resonance frequency of a r.f. cavity containing the discharge capillary. The values are given in figure 2. Also are shown the mean T_e values calculated from the similarity law (33) with two different assumptions : either pure H_2 or pure H gas. Due to the low degree

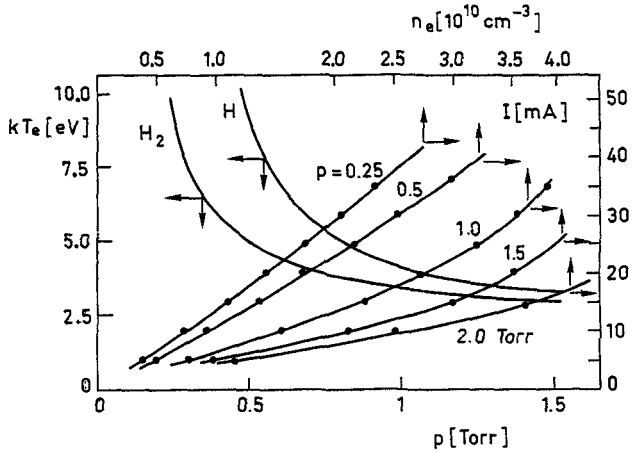

Fig. 2. — Mean electron temperature T_e as a function of pressure p for a glow discharge in pure H_2 or pure H gas, calculated from the similarity law. Also are shown the measured mean electron density n_e as a function of plasma current I at different pressures p. R is 2 mm, after [19].

of dissociation the H_2 curve is the more probable one. One further sees that the similarity law (35) with $n_e \propto I$ is approximately verified in the range of pressures employed.

By pumping successively the $n = 3$, 4 and 5 states of atomic hydrogen by means of a short laser pulse (duration $\sim$ 4 ns) at different values of I and p and then observing the intensity decay of H_α, H_β and H_γ lines, the effective deexcitation frequencies ν_3, ν_4 and ν_5 could be determined. Results are shown in figure 3. ν_n ($n = 1$, 2, 3) increases with p. One would also expect an increase of ν_n with I, i.e. an increase with n_e; however, the contrary is the case. The measurements can be described by the following linear dependence :

$$\nu_n(p, I) = A_n + B_n(I)\, p \qquad (37)$$

A_n represents the effective spontaneous deexcitation frequency of level with principal quantum number n :

$$A_n = \sum_{m<n} A_{mn}\, A_{mn} \qquad (38)$$

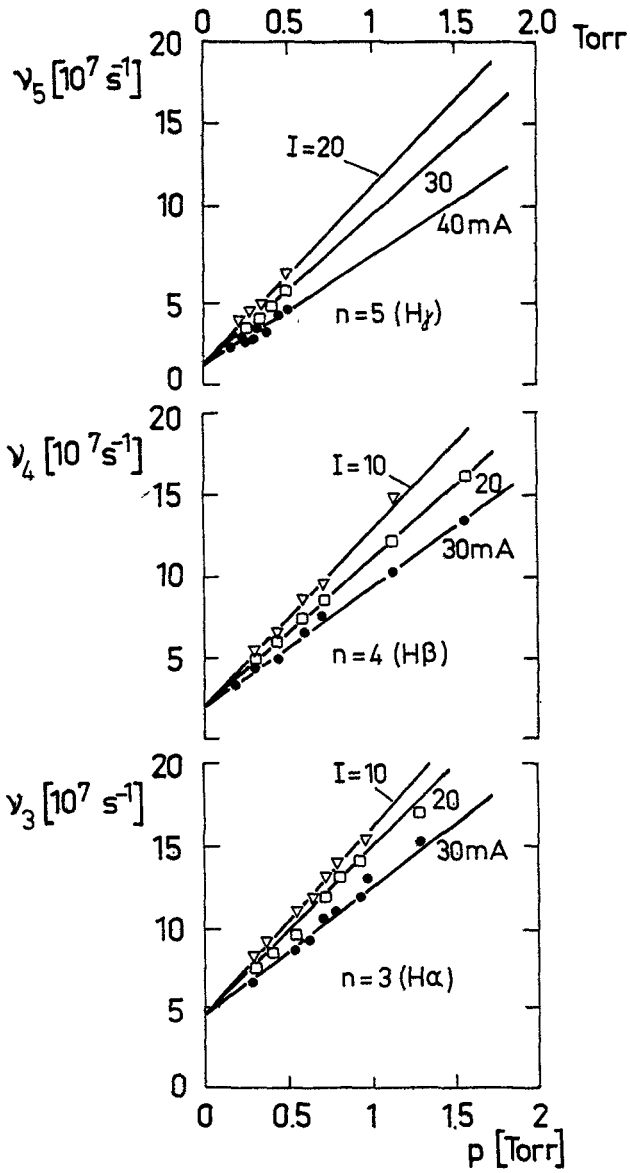

Fig. 3. — Effective de-excitation frequency ν_n of the atomic hydrogen levels $n = 3$, 4 and 5 as a function of pressure p at different plasma currents I, after [19].

where A_{mn} are the optical escape factors. Extrapolation of the measured curves to $p = 0$ yields A_n — values consistent with the assumptions that the $Ly\alpha$ and $Ly\beta$ lines are completely reabsorbed and that only 40 % of the $Ly\delta$ intensity escapes from the plasma; the other lines being optically thin.

For ν_n we can write the following dependence (where three-body collisions are neglected due to the relatively low pressures) :

$$\nu_n(p, I) = A_n + n_{\text{H}} \sum_{n \neq n'} \beta_{nn'} + n_{\text{H}_2} \sum_{\zeta} \gamma_{n\zeta} + \\ + n_e \sum_{n \neq n'} \varepsilon_{nn'} \qquad (39)$$

where the rate coefficients $\beta_{nn'}$, $\gamma_{n\zeta'}$, $\varepsilon_{nn'}$ refer to the following reactions :

• *Excitation (de-excitation)* due to atomic collisions

$$H(n) + H(1) \xrightarrow{\beta_{nn'}} H(n') + H(1) + \Delta E \quad (40a)$$

or associative ionisation

$$H(n) + H(1) \xrightarrow{\beta_{nn'}} H_2^+ + e + \Delta E . \quad (40b)$$

• *Excitation transfer* due to atom-molecule collisions

$$H(n) + H_2(n, \Omega, v, N) \xrightarrow{\gamma_{n\zeta}} H(n') + H_2(n'', \Omega'', v'', N'') + \Delta E . \quad (41)$$

• *Electronic excitation* (de-excitation)

$$H(n) + e \xrightarrow{\varepsilon_{nn'}} H(n') + e + \Delta E \quad (42)$$

where $\zeta = (n, \Omega, v, N)$ represents the ensemble of quantum numbers which characterize an excited molecule.

The fact that induced fluorescence is only observed from the pumped levels leads to the conclusion that the processes (40*a*) and (42) are unefficient under the chosen experimental conditions (this was also verified experimentally). Also the reaction (40*b*) could be neglected. Thus, the eq. (39) can be approximated by

$$\nu_n(p, I) \approx A_n + n_{H_2}(p, T_0, I) \sum_\zeta \gamma_{n\zeta}(T_0) \quad (43)$$

where the reaction coefficient $\gamma_{n\zeta}$ depends only on the relative translation energy between atoms and molecules, i.e. on the gas temperature T_0.

The gas temperature T_0 was measured with a thermo-couple ($T_0 \simeq 320$ K independent of p and I). Owing to the very low degree of ionisation one has :

$$p \simeq (n_{H_2} + n_H)\, kT_0 . \quad (44)$$

At a given pressure p, a decrease of n_{H_2} must be compensated by a corresponding increase of n_H. The decrease of ν_n with increasing I (see Fig. 3) is now compatible with the relation (43) under the assumption that an increase of I, i.e. an increase of n_e (see Fig. 2) lowers the molecular density n_{H_2} due to increased dissociation according to the reaction :

$$H_2(X\,^1\Sigma_g^+) + e^- \xrightarrow{\delta_M} H(1) + H(1) + e^- + \Delta E . \quad (45)$$

The atoms are mainly formed in the ground state $n = 1$. The rate equation for the reaction (45) is

$$\frac{\partial n_1}{\partial t} = 2\, \delta_M n(H_2)\, n_e - \nu_1\, n_1 \quad (46)$$

where ν_1 represents a loss coefficient. A second collision is necessary for excitation into the levels $n > 1$:

$$H(1) + e^- \xrightarrow{\varepsilon_{1n}} H(n > 1) + e^- + \Delta E . \quad (47)$$

The rate equation for the excited hydrogen atoms $n > 1$ is given by

$$\frac{\partial n_{n>1}}{\partial t} = \varepsilon_{1n}\, n_1\, n_e - \nu_{n>1}\, n_{n>1} . \quad (48)$$

For the stationary discharge ($\partial/\partial t = 0$), the number density of the excited hydrogen atoms must therefore be proportional to n_e^2 :

$$n_{n>1} = 2 \frac{\delta_M\, \varepsilon_{1n}}{\nu_1\, \nu_{n>1}} n(H_2)\, n_e^2 . \quad (49)$$

As long as the degree of dissociation remains low (< 5 %) the formation of atomic hydrogen will not affect the H_2 concentration very much, whereas the atom density can strongly vary with n_e.

A measurement of the intensity of atomic and molecular lines as a function of n_e at a given pressure confirmed that the intensity of the molecular lines varies at low degrees of dissociation linearly with n_e whereas the one of the atomic lines increases with n_e^2. It has thus been proved that the reaction (41) can explain the experimental features.

The results of the figure 3 permit to determine $\sum_\zeta \gamma_{n\zeta}$. Putting $\sum \gamma_{n\zeta} = \langle \sigma(n) \rangle_{H-H_2} \langle v \rangle$ where $\langle v \rangle$ is the mean relative velocity between H and H_2 particles yields the mean effective cross-sections listed in table 1.

Table 1. — *Mean effective cross-section* $\langle \sigma(n) \rangle_{H-H_2}$ *for collisional de-excitation of excited hydrogen atoms by* H_2 *molecules after* [19]. *The values from* [20] *refer to a collision experiment in which* H *was excited by* 40 keV *electrons passing through* H_2 *gas.* $\langle \sigma \rangle$ *is in* Å^2.

	$n = 3$	$n = 4$	$n = 5$
$\langle \sigma(n) \rangle_{H-H_2}$ [19]	156 ± 3	145 ± 4	146 ± 5
$\langle \sigma(n) \rangle_{H-H_2}$ [20]	76 ± 3	32 ± 3	8.9 ± 0.7

The experimental values obtained from the glow discharge plasma are almost independent of n which is not the case for the collision experiment. It might be that the more abundant vibrationally-rotationally excited molecules in a discharge plasma are responsible for this discrepancy.

Dubreuil and Catherinot [19] also measured the decay of the fluorescence light of a number of molecular lines after pumping of the atomic states. The molecular fluorescence intensity is proportional to the atomic fluorescence intensity (see Fig. 4) in agreement with reaction (41). They could especially determine the reaction coefficients $\gamma_{n\zeta}$ for molecules in the electronic ground and in the excited metastable state $H_2(a\,^3\Sigma_g^+, v' = 0, N' = 4)$ according to :

$$H(n) + H_2(X\,^1\Sigma_g^+, v = 0, N) \rightarrow H(1) + H_2(n', \Omega', v', N') + \Delta E \quad (50a)$$

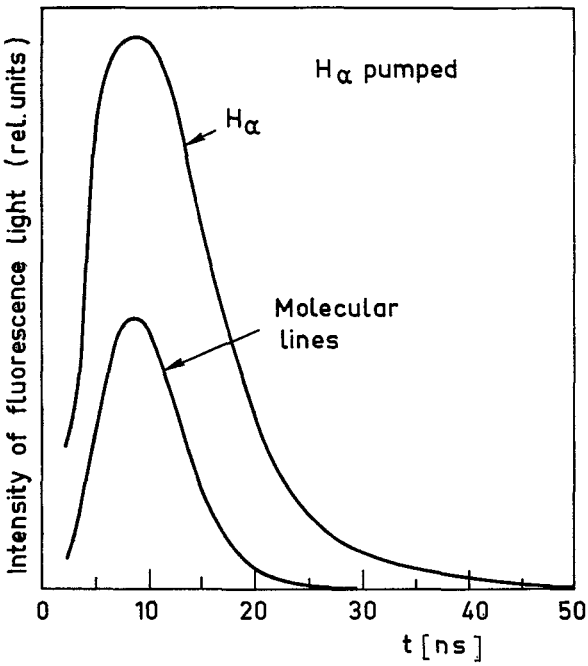

Fig. 4. — Fluorescence light of atomic and molecular lines after laser pumping of the atomic level $n = 3$ of hydrogen, after [19].

$$H(3) + H_2(a\,^3\Sigma_g^+, v = 0, N = 4) \rightarrow H(2) + H_2(e\,^3\Sigma_u^+, v' = 2, N' = 5) - 16\ cm^{-1} \quad (50b)$$

which are two special reactions of type (41). They also determined cross-sections for rotational relaxation induced by collisions with atoms and molecules according to the reactions

$$H_2(n, \Omega, v, N) + H(n = 1) \rightarrow H_2(n, \Omega, v, N') + H(n = 1) + \Delta E \quad (51a)$$

$$H_2(n, \Omega, v, N) + H_2(X\,^1\Sigma_g^+) \rightarrow H_2(n, \Omega, v, N') + H_2(X\,^1\Sigma_g^+) + \Delta E. \quad (51b)$$

It was found that the transitions with a change of $\Delta N = \pm 1$ in the rotational quantum number were much more efficient than those with $\Delta N > 1$ indicating that Ω is not further a good quantum number for the electronic states involved. (The usual selection rule for homonuclear molecules treated in the frame of the Born-Oppenheimer method is $\Delta N = \pm 2$.)

The experimental work of Dubreuil and Catherinot together with theoretical calculations by Capitelli *et al.* [21], Cacciatore *et al.* [22] and Capezzuto *et al.* [23] has led to a better comprehension of the microscopic processes which determine the properties of the hydrogen glow discharge; together with older known work the situation may be summarized as follows :

• *Formation of ion-electron pairs* : The H_2 molecules deliver the bulk of the positive ions and electrons by direct ionisation from the electronic ground level or via a two-step process with the metastable and pseudo-metastable levels as intermediate states :

$$H_2 + e^- \rightarrow H_2^+ + 2\,e^-. \quad (52)$$

According to present knowledge the production rate of H^+ ions via the two-step process

$$H_2 + e^- \rightarrow H_2^+ + 2\,e^- \rightarrow H + H^+ + 2\,e^- \quad (53)$$

is smaller by several orders of magnitude. At higher degrees of dissociation the process $H + e^- \rightarrow H^+ + 2\,e^-$ may play a role (this is the process analogue to reaction (47) for the excitation of atomic levels).

• *Dissociation* : Obviously two different processes are responsible for dissociation; first, dissociation by electron impact :

$$H_2(X\,^1\Sigma_g^+) + e^- \rightarrow H(1) + H(1) + e^-. \quad (54a)$$

The electron rises the molecule to the first repulsive state ($^3\Sigma$), followed by dissociation; second, dissociation due to collision of two vibrotational excited molecules, the excitation arising from electronic collisions [21-23] :

$$H_2(e^{-1}\Sigma_g^+, v = 0, N) + e^- \rightarrow H_2(X\,^1\Sigma_g^+, v', N') + e^-$$
$$H_2(X\,^1\Sigma_g^+, v', N') + H_2(X\,^1\Sigma_g, v'', N'') \rightarrow H(1) + H(1) + H_2^*. \quad (54b)$$

• *Formation of excited atoms* is essentially due to electronic collisions of the atom in the ground state :

$$H(1) + e^- \rightarrow H(n) + e \quad (55)$$

after the molecule has been dissociated.

• *Formation of excited molecules* : Two processes are possible, namely direct excitation by electron collisions :

$$H_2(X\,^1\Sigma_g^+) + e \rightarrow H_2^* \quad (56a)$$

and excitation transfer due to molecule-atom collisions :

$$H_2(X\,^1\Sigma_g^+) + H(n) \rightarrow H_2(n, \Omega', v', J') + H(1). \quad (56b)$$

• *Destruction of excited atoms and molecules* is mainly via radiative transitions and due to collisions with atoms and molecules in the ground state :

$$H^* \rightarrow H^{*\prime} + h\nu \quad (57a)$$
$$H^* + H_2 \rightarrow H^{*\prime} + H_2^*$$

$$H_2^* \rightarrow H_2^* + h\nu \quad (57b)$$
$$H_2^* + H \rightarrow H_2^{*\prime} + H$$
$$H_2^* + H_2 \rightarrow H_2^{*\prime} + H_2$$

• *Destruction of ions* (H^{2+}, H^+) is mainly due to diffusion to the walls (ambipolar diffusion) followed by recombination on the walls. This process is only dominant in a limited range of p ($\sim 10^{-1}$ to 10 torr), or R ($\sim$ 1 mm to 100 mm) and of I ($\sim 10^{-4}$ to 1 A).

The measurements showed further that the electrons contribute little to the transfer of energy between excited states (collisional excitation, de-excitation negligible).

3.3 THE GLOW DISCHARGE IN NITROGEN GAS. — An experimental study of Polak *et al.* [24] led to the result that the molecular ionisation rates for all regimes of a glow discharge in N_2 gas (I = 5 to 75 mA ; R = 1.6 cm, p = 0.6 to 6.3 torr) must lie above the values computed under the assumption of direct ionisation by electron impact (see Fig. 5).

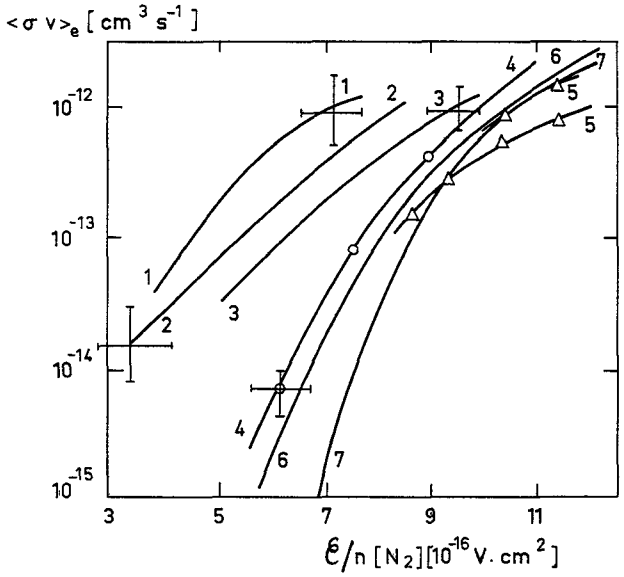

Fig. 5. — Rate coefficient $\langle \sigma_1 v \rangle = S$ for volume ionisation in a glow discharge in pure N_2 gas as a function of $\mathcal{E}/n$. Curves 1 to 5 deduced from measurements : 1) i = 9.5 mA/cm^2 ; 2) i = 3.8 mA/cm^2 ; 3) i = 1.25 mA/cm^2 ; 4) i = 0.63 mA/cm^2 ; 5) from swarm experiments ; 6) calculation for direct ionisation after reaction [40*a*] with T_v = 8 000 K ; 7) the same with vibrational temperature T_v = 300 K. After [24]. Experimental error bars are ± 100 %.

Impurities could not be made responsible for the large discrepancies between theoretical and experimental values. From these and other observations the authors conclude that the ionisation mechanism under glow discharge conditions occurs via the following processes :

• *Direct ionisation* (X is the electronic ground state)

$$N_2(X) + e^- \rightarrow N_2^+ + 2\,e^- . \qquad (58a)$$

• *Stepwise electronic ionisation* (Z is an excited electronic state)

$$N_2(X) + e^- \rightarrow N_2(Z) + e^- \rightarrow N_2^+ + 2\,e^- \qquad (58b)$$

• *Electronic excitation followed by ionisation due to molecule-molecule collisions* :

$$N_2(X) + e^- \rightarrow N_2(Z) + e^- \qquad (59a)$$

$$N_2(Z) + N_2(Z') \rightarrow N_2^+ + N_2 + e^- \qquad (59b)$$
$$(E_Z + E_{Z'} \geqslant E_{ion}) \hookrightarrow N_4^+ + e^-$$

$$N_2(Z) + N_2(X, v) \rightarrow N_2^+ + N_2 + e^- \qquad (59c)$$
$$(E_Z + E_{X,v} \geqslant E_{ion}) \hookrightarrow N_4^+ + e^- \qquad (59d)$$

where E_Z, $E_{Z'}$, $E_{X,v}$ and E_{ion} denote the excitation and ionisation energies respectively. Further the following transformations seem to be likely :

$$N_2^+ + 2\,N_2 \rightleftharpoons N_4^+ + N_2 ; \qquad (60a)$$

$$N_4^+ + N \rightarrow N^+ + 2\,N_2 . \qquad (60b)$$

• *The destruction of the ions* is mainly due to ambipolar diffusion followed by recombination on the walls :

$$2[N^+ + e^-] \xrightarrow{\text{wall}} 2\,N \rightarrow N_2 \qquad (61a)$$

$$[N_2^+ + e^-] \xrightarrow{\text{wall}} N_2 \qquad (61b)$$

$$[N_4^+ + e^-] \xrightarrow{\text{wall}} 2\,N_2 . \qquad (61c)$$

It has experimentally been observed that the N_4^+ concentration decreases with increasing current. This effect is interpreted as being due to a decrease of the N_2 density, because of an increase of dissociation with increasing electron density (because n_e is proportional to I) (see eq. (35)). According to the reactions (59*a*)-(59*d*) the production rate of N_4^+ should be proportional to $n_{N_2}^2 n_e^2$. This dependence has experimentally not yet been demonstrated.

In this context the theoretical work of Winkler and Pfau [26-27] on the glow discharge in N_2 gas should be mentioned. They calculated electron velocity distribution functions, collision frequencies, energy loss rates, direct ionisation frequencies and other quantities related to atomic processes. Capitelli and Dilonardo [25] (see also [22]) calculated the non-equilibrium excitation and dissociation of nitrogen molecules in electrical discharges.

The findings of Polak *et al.* [24] lead to the question if cluster ions could not play a role in glow discharge plasmas of other molecular gases ?

It should finally be mentioned that Engelke [28] considered dissociating collisions in the frame of the Schottky theory.

3.4 THE GLOW DISCHARGE IN ATOMIC GASES ; THE CONSTRICTION PHENOMENON. — According to the different values of p and I, a glow discharge appears visually as either a diffuse-homogeneous, a diffuse-striated, a constricted striated or a constricted-homogeneous plasma column. Figure 6 shows the existence regions of those types of discharges for neon. Similar curves for the other rare gases may be found

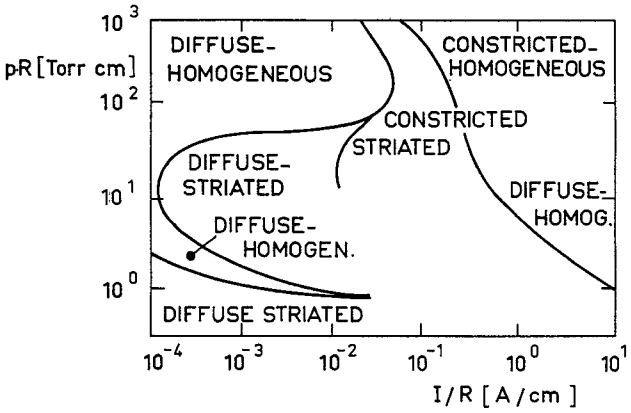

Fig. 6. — Existence diagram of the different column states in the case of a discharge in neon gas; p = filling pressure; I = discharge (plasma) current; R = tube radius; after [29, 36].

in [29]. When one goes for instance from low to higher values of I (for given values of pR) a diffuse-homogeneous discharge suddenly constricts. This constriction is accompagnied by a sharp decrease of the electric field strength $\mathcal{E}$ as shown in figure 7. If I changes from the higher to the lower values, the discharge returns to the diffuse state at a value of I slightly different from the one which was obtained for the opposite direction. One has a kind of hysteresis which increases with decreasing pressure. This constriction phenomenon has been known for a long time, however, even systematic theoretical studies have not yet led to a satisfactory description of this effect. It is interesting to see what a progress has been achieved during the last years by including various atomic and molecular processes in the theoretical model.

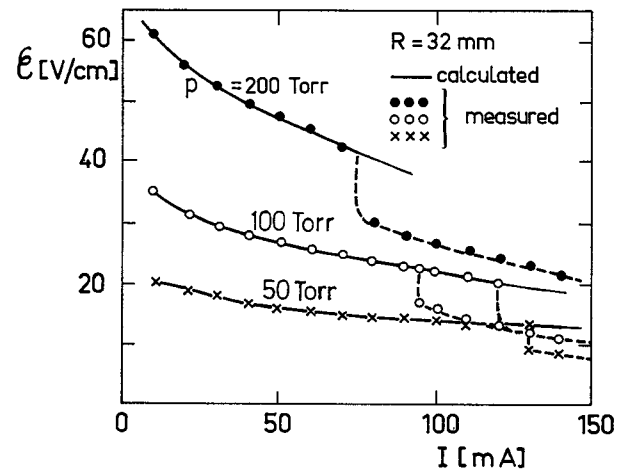

Fig. 7. — Measured electric field strength as a function of current I for a discharge in neon. R = 32 cm, ● 200 torr, ○ 100 torr, × 50 torr, — calculations, --- constricted discharge measured. After [36].

In the following we refer first to the work of Wojaczek who studied in a series of papers the constriction by making different theoretical assumptions. In [30] the following assumptions were made :

1. The ionisation coefficient is equal to a modified *Maxwell coefficient* (see also eq. (23)) and has the form

$$S' = S_M \frac{b}{B} e^{-KB} \tag{62}$$

where S_M refers to a Maxwell distribution. b and K are constants, B is $\sim 1/n_e$.

2. Superelastic collisions are neglected.
3. All ion-electron pairs diffuse to the walls due to ambipolar diffusion. They recombine on the walls.
4. Electron temperature T_e independent of r.
5. Gas temperature T_0 independent of r.
6. Neutral gas density constant across r.
7. Volume recombination is neglected.

The radial distribution of n_e is then described by the equation :

$$D_a \frac{1}{r} \frac{\partial}{\partial r} \left(r \frac{\partial}{\partial r} n_e \right) + S_M n_e \frac{b}{B} e^{-KB} n_e = 0 . \tag{63}$$

The solutions show a strong constriction with increasing values of $C_0(r = 0) = KB_0$, where B_0 is the value of B on the axis. The relative distribution $n_e(r)/n_e(0)$ is shown in figure 8. The curve B represents the Bessel function. Similar curves have been obtained by Albrecht *et al.* [31].

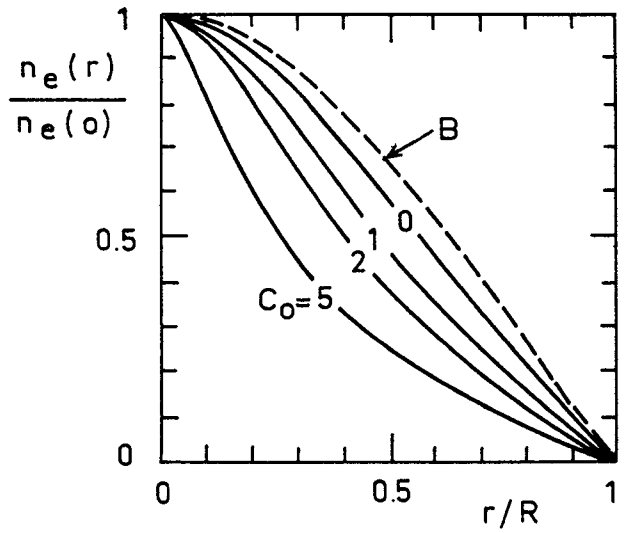

Fig. 8. — Relative radial distribution of the electron density $n_e(r)$ calculated from eq. (63), for different values of the constant C_0 on the axis. The curve B represents the Bessel function which is obtained when $b/B \exp(-KB) = 1$. After [30].

In a subsequent paper Wojaczek [32] assumes instead of the condition 5 above, that the gas temperature depends on r via heat conduction. All other

assumptions remain unchanged. Now $n_e(r)$ and $T_0(r)$ are determined by the following equations :

$$\frac{1}{r}\frac{\partial}{\partial r}\left(D_a r \frac{\partial}{\partial r} n_e\right) + \frac{1}{r}\frac{\partial}{\partial r}\left(r n_e D_a \frac{1}{T_0}\frac{\partial T_0}{\partial r}\right) + + S_M n_0 n_e \frac{b}{B} e^{-KB(n_e)} = 0 \quad (64)$$

$$\frac{1}{r}\frac{\partial}{\partial r}\left(r \mathcal{K} \frac{\partial T_0}{\partial r}\right) - \Omega = 0 \quad (65)$$

where $\mathcal{K}$ is the thermal heat conduction and $\dot{\Omega} = i\mathcal{E}$ is the source term (heating of the neutral gas by electron collisions). Compared to the solutions of eq. (63), the radial dependence of T_0 practically does not change the results in the range of interest.

A comparison with measurements for argon shows that the experimentally observed constriction is usually stronger than predicted by the model.

In a next paper [33] he assumed that also T_e depends on r. The solution of the corresponding differential equations leads to the conclusion that the radial dependence of T_e is of little consequence for the constricted discharge.

In a last paper [34] the calculations are based on the same assumptions 1 to 6 as in the first paper [30], however, instead of the condition 7 volume recombination is now included in the model (assumed to be independent of r). Instead of eq. (63) the following differential equation has to be solved :

$$D_a \frac{1}{r}\frac{\partial}{\partial r}\left(r \frac{\partial}{\partial r} n_e\right) + S_M n_0 n_e \frac{b}{B} e^{-KB(n_e)} - \alpha n_e^2 = 0 . \quad (66)$$

The results lead with recombination to a stronger constriction of the $n_e(r)$ distribution than without recombination, but the theoretical model gives still too wide n_e — distributions compared to the experiments. Also the theoretically calculated electric field strength $\mathcal{E}$ does not agree with the measured ones. Taking recombination into account leads to an increase of $\mathcal{E}$ instead of a lowering as it is observed for the constricted column (see. Fig. 7).

A much more sophisticated collisional-radiative model for a glow discharge in neon and in argon has been set up and solved by Smits and Prins [35-36]. The following assumptions were made :

1. The molecular ion density (for instance $n(Ne_2^+)$) is much greater than the atomic ion density (for instance $n(Ne^+)$). The latter can therefore be neglected; the quasi-neutrality condition gives $n_e = n(Ne_2^+)$.

2. Direct ionisation is negligible with respect to stepwise ionisation. This stepwise ionisation, i.e. the ultimate formation of Ne_2^+ ions, proceeds via associative ionisation $Ne^* + 2\,Ne \rightarrow Ne_2^+ + Ne + e^-$ (see Fig. 9 and ref. [37]).

3. The diffusion of the charged particles is governed by ambipolar diffusion.

4. Diffusion of excited particles is neglected.

5. Radiative transfer is taken into account by means of Holstein's radiative escape factor.

6. The radial dependence of the gas temperature is taken into account by solving the corresponding heat transfer equation for the neutral gas.

7. Volume recombination is taken into account in the form of dissociation recombination. For neon the following recombination coefficient has been chosen (see p. 2232 of [37])

$$\alpha = \frac{2.5 \times 10^{-8}}{(kT_e)^{1/2}}\left[1 - \exp\left(\frac{-900}{kT_0}\right)\right] \text{cm}^3\,\text{s}^{-1} \quad (67)$$

where kT_0 is in eV.

8. Superelastic collisions have been neglected.

The various reaction channels which have been taken into account are shown in figure 9 for neon. The associative ionisation process

$$Ne^* + 2\,Ne \rightarrow Ne_2^+ + Ne + e^-$$

is only effective for particles belonging to the groups III and IV. The axial field strength (axially constant) and the velocity distribution function for the electrons have been calculated including elastic electron-electron, elastic electron-atom, and inelastic electron-atom collisions. The electron-electron collisions ensure

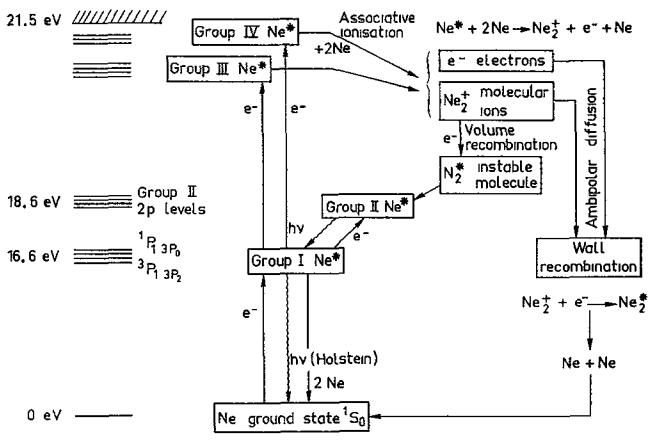

Fig. 9. — Atomic and molecular processes which have been taken into account in the collisional-radiative model of a glow discharge in neon gas, after [35, 36].

that $f(E)$ tends to a Maxwellian at high electron densities (but never reaching it). The inelastic and elastic electron-atom collisions lead to a depopulation of the tail of $f(E)$ compared to a Maxwell distribution. Figure 10 shows a calculated distribution function.

The main results of the model calculations compared to measurements are :

a) For the diffuse discharge, the calculated radial

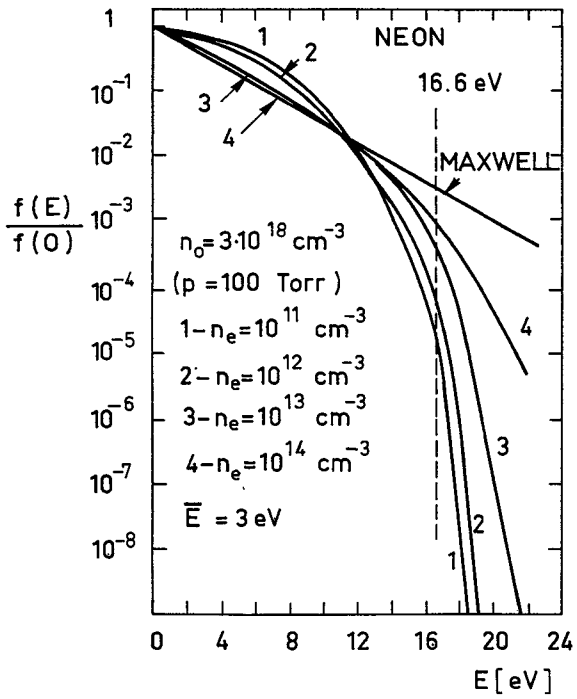

Fig. 10. — Calculated velocity distribution function $f(E)$ for electrons moving in a neon glow discharge plasma under the influence of an applied electric field at different electron densities. The mean translational energy is $\bar{E} = 3$ eV, the neutral gas density corresponds to a pressure of $p = 100$ torr. After [36].

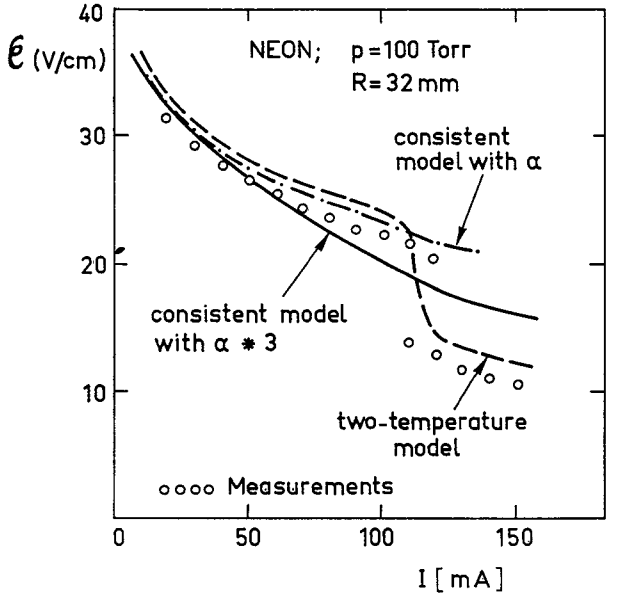

Fig. 11. — Influence of volume recombination α and of temperature model on the constriction phenomenon. —.—.— with α given by eq. (67) and consistently calculated velocity distribution function $f(E)$; —— the same but with three times larger value for α; --- two-temperature model for the electrons; OOOO measured values. After [36].

distributions of n_e and of the excited states agree relatively well with the measurements. This is not the case for the constricted discharge.

b) For the diffuse discharge the calculated electric field strength $\mathcal{E}$ also agrees with the measurements (see the examples given in figures 7 and 11). However, the sudden decrease of $\mathcal{E}$ for the constricted discharge could not be reproduced.

The authors have changed several parameters and found that $\mathcal{E}$ decreases more rapidly with current I when α is increased. Figure 11 shows an example where α was increased by a factor of three. A much better transition from the « diffuse » to the « constricted » $\mathcal{E}$-values could be obtained by increasing in the Boltzmann equation, which served for calculating $f(E)$ — the Coulomb terms by a factor of six. A *nearly sudden transition* from one regime to the other could be obtained by chosing a two-temperature model. Instead of using the calculated distribution function the authors chose a Maxwellian distribution with a bulk temperature T_0 on which another Maxwell distribution — corresponding to an electron density-dependent tail temperature T_t — was superposed. The following ratio between T_t and T_0 was assumed :

$$\frac{T_t}{T_0} = \frac{C_2 + n_e/n_0}{C_1 C_2 + n_e/n_0}. \qquad (68)$$

Chosing $C_1 = 2.66$, $C_2 = 6.5 \times 10^{-7}$ the constriction phenomenon occurs at $I \simeq 120$ mA as is observed experimentally (see Fig. 11).

From a theoretical point of view this method is unsatisfactory. However, the fact that constriction can be obtained when a group of energetic electrons is included in the model has led the authors to propose another mechanism which might be responsible for constriction : the formation of energetic electrons caused by an ionisation instability in the form of a striations generating process.

It should be mentioned, however, that the tail of $f(E)$ can also be populated by superelastic collisions which have been neglected in the model. For instance for neon the rate of electronic deexcitation can become important due to the metastability of the first excited 3s-levels and the quasi-metastability of the 3p-levels (as a result of strong resonance reabsorption). If one includes in the model diffusion of this group of levels it might be that a kind of spatial excitation-deexcitation relaxation is build up which could be capable in producing a group of hot electrons in the tail of the velocity distribution function and which is obviously needed in order to explain the observed features. The assumption of diffusion of excited states would also be in agreement with the experimental fact that the observed line emission shows a larger radial profile than do the model calculations provided the radiating levels are sufficiently coupled to the metastable and quasi-metastable levels through collisional processes.

4. **Negative ion plasmas.** — 4.1 GENERAL CONSIDERATIONS. — Until now, we have only considered positive ion-electron plasmas. However, under appropriate conditions, one can produce plasmas containing

a relatively large amount of negative ions. For some gases, especially those containing halogens, a quasi-negative ion plasma can be produced, the electron density being negligible. Negative ions containing plasmas are not only of fundamental interest, they play a great role in astrophysics and are of great importance in electric circuit breakers. They may become important in the production of energetic neutral beams for plasma heating (neutral beam injection in Tokamak plasmas). Also the diffusion and wave properties of negative ion plasmas are of interest, since electron induced ambipolar fields no longer dominate the diffusion characteristics, and the shielding of low-frequency fields by electrons become increasingly unefficient with higher densities of negative ions. For a pure electronegative gas the similarity laws are different from the ones given above for pure electron-positive ion plasmas.

Negative ions can be produced in many different ways. In molecule-free plasmas, there exists only one single mechanism, that is the attachment of free electrons to neutral atoms with positive electron affinity. The energy liberated in this process is emitted in form of a photon $h\nu$ which produces the electron affinity continuum. The absorption of continuous radiation by negative ions causes photo-detachment of the bound electron. Thus,

$$A + e^- \rightleftarrows A^- + h\nu . \qquad (69)$$

In astrophysical objects, these two reactions are of considerable interest when A represents a hydrogen, an oxygen, or a nitrogen atom. The continuum opacity of the Sun's atmosphere originates from H^- absorption, the O^- and N^- ions play a role in the sunlit ionosphere.

The electron affinity (or attachment) continua are currently observed in emission from low current arcs at atmospheric pressure and in shock-tube experiments provided the optical depth does not exceed the value one to two (for higher optical depths, the arc emits as a black-body). For further details, the reader is referred to the recent papers [39-44].

The physics of the negative ions is not yet well understood. There should exist a whole series of excited levels with energies close to those for the excited H-atom [45]. Until now, the experimental search for these states has led to negative results [46]. An exception is the experimental confirmation of the 1s 2p ^{1}P shape resonance of H^- at $\lambda = 1\,130$ Å [46-48] predicted by Macek and Burke [49], see also [50].

Recent measurements of the detachment cross-sections for the reaction $e^- + H^- \rightarrow H + 2\,e^-$ have led to the conclusion that the observed order of magnitude ($\sigma \lesssim 4.10^{-15}$ cm^2) was insufficient for the process to be important in astrophysics. It seems to be more likely that the destruction of H^- in cold stellar atmospheres is primarily due to associative detachment [51, 52] :

$$H^- + H \rightarrow H_2^- \rightarrow H_2(X\,^1\Sigma_g^+, v, N) + e^- . \qquad (70)$$

New calculations of the cross-section for reactions (70) which are capable to populate rotational-vibrational states have been published by Bieniek and Dalgarno [53].

There are also experimental indications from laboratory experiments that there might exist reaction channels for the formation of H^- which have still to be identified.

4.2 FORMATION OF H^- IN A LOW-PRESSURE PLASMA. — Doucet and collaborators [54] produced a hydrogen plasma in a kind of cylindrical multipole and measured the negative ion density by means of an electrostatic probe (plasma volume $\sim$ 50 l, filling pressure $\sim 10^{-3}$ torr). It was found that the H^- density continuously increased with pressure, and attained values of $\sim 3.10^9$ cm^{-3}, that is 30 % of the positive ion density. The measured values are graphically shown in figure 12. The figure also shows values calculated from the steady-state equation including the following processes with $v = 0$ in eqs. (71a, b) :

- *Dissociative electron attachment*

$$e^- + H_2(X\,^3\Sigma_g, v) \rightarrow H_2^-(^2\Sigma_u^+) \rightarrow H(1s) + H^- \qquad (71a)$$

$$e^- + H_2(c\,^3\pi_u, v) \rightarrow H_2^-(^2\pi_u) \rightarrow H(2p) + H^- . \qquad (71b)$$

- *Polar dissociation*

$$e^- + H_2 \rightarrow H^+ + H^- + e^- . \qquad (72)$$

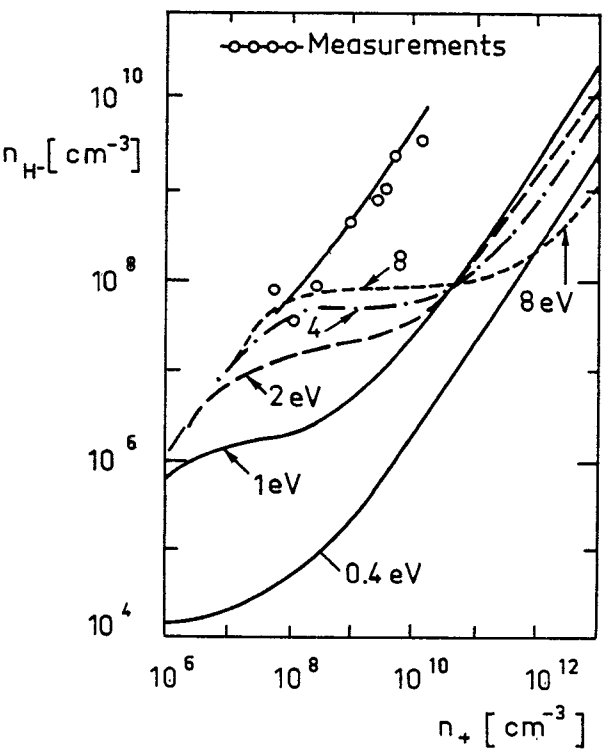

Fig. 12. — Negative ion density $n(H^-)$ as a function of positive ion density n_+, after [54]. The electron temperature is taken as curve parameter. H^+ ions are assumed to be negligible, thus $n_+ = n(H_2^+)$.

• *Dissociative recombination*

$$e^- + H_2^+ \rightarrow H^- + H^+ \qquad (73a)$$

$$e^- + H_3^+ \rightarrow H^- + H_2^+ . \qquad (73b)$$

• *Collisional electron detachment*

$$e^- + H^- \rightarrow e^- + H + e^- . \qquad (74)$$

• *Mutual neutralisation*

$$H^- + H_2^+ \rightarrow H_2 + H . \qquad (75)$$

and

• *Diffusion*

From figure 12 one sees that the measured values are 100 times higher than the calculated ones at the highest plasma density. At the present, there is no satisfactory explanation for this large discrepancy. Photodetachment measurements allowed to determine the H^- density as a function of n_e. For a plasma with the following parameters $n(H_2) \approx 2.10^{14}$ cm^{-3}, $n_e = 1.7.10^9$ to $1.1.10^{10}$ cm^{-3}, $kT_e \approx 0.1 \ldots 0.4$ eV, a dependence $n(H^-) \propto n_e^3$ was found [55-56]. At maximum density, a ratio of $n(H^-)/n_e \approx 0.35$ was observed. It is assumed that one (or both) of the reactions (71*a*), (71*b*) are responsable for the H^- production. Also the process (73*b*) cannot completely be excluded. The reactions in H^- and D^- containing plasmas have been reviewed in [57].

4.3 ELECTRIC CIRCUIT-BREAKERS ; RECOMBINATION OF SF_6 PLASMAS.—High-power electric circuit breakers are used to interrupt high currents under medium- or high-voltage conditions. Such switchgears contain sulphur hexafluoride (SF_6) gas because of its outstanding dielectric properties under high-voltage and high-temperature conditions. A circuit-breaker consists of one or two axially movable electrodes in a SF_6 containing vessel. The vessel consists of two electrode chambers connected by a channel (nozzle). During breaker operation a high pressure difference is maintained between the chambers.

In the normal position, the electrodes are in contact and the current can flow through. When the current is to be interrupted, the electrodes are separated. An arc is established which burns through the nozzle. The arc is submitted to a strong gasblast of SF_6 which cools the ionised gas. When the current goes through zero, the plasma has a temperature of approximately 10^4 K, the gas is fully dissociated and partially ionised, the thermodynamic state is close to L.T.E. The main constituents are F, S, S^+ and electrons [58-59]. Close to and at current zero, a strong ion-electron recombination begins accompanied by the formation of negative F^- ions. Also molecules are formed. When the high-voltage reappears in the next half period, the electrons must have disappeared in order to avoid re-arcing. The current interruption was successful when the gas has withstood the full voltage. The rapid formation of negative ions by electron attachment is essential for the extinguishing capabilities of the SF_6 plasma. Industry builds current breakers which are capable to interrupt currents of the order of 75 kA per breaker unit and which can withstand voltages of the order of 70 to 100 kV. Connected in series, circuit-breakers are applied for voltages of the order of 500 kV. For further details, the reader is referred to [60-69].

The physical properties of the recombining SF_6 plasma with and without an applied electric field are not yet well understood. Both experiments and theoretical considerations have led to the conclusion that the essential reason for electrical breakdown or re-arcing of a hot SF_6 gas is the presence of negative ions of the order of 10^{13} cm^{-3} at a temperature of about 2 500 K. The dielectric properties depend on the reaction rate for electron detachment followed by electron avalanches under the influence of the applied electric field and the rate for electron attachment. The temporal evolution of the plasma composition during recombination is still unknown to a large extent.

It should in principle be possible to calculate the temporal evolution of the plasma composition from a system of coupled equations for the particle densities, momenta and energies. At constant plasma temperature, the physical situation can be described as follows : recombination will first lead to a decrease of total pressure with a rate according to (see eqs. (8) to (13))

$$\left(\frac{\partial p}{\partial t}\right)_T = \sum_s \left(\frac{\partial p_s}{\partial t}\right)_T = kT \sum_s \left[\frac{\partial n_s}{\partial t}\right]_{\substack{\text{coll.} \\ \text{rad.}}} \qquad (76)$$

Thus, a pressure difference is built-up which leads to a general diffusion and mass flow of the plasma (eqs. (14) (16)) in order to re-establish the pressure. This mass motion is accompanied by a transport of energy (eq. (19)). In order to make the problem mathematically tractable many simplifying assumptions have to be made. Also the many reaction cross-sections must be known, which is not the case at present.

The physical situation becomes much simpler when a homogeneous recombining plasma volume at constant pressure is considered, which might be submitted to a simultaneous temperature variation. A simplified rate equation for the species s can then be obtained in the following way : the species s contributes to the pressure drop with a rate

$$\left(\frac{\partial p_s}{\partial t}\right)_T = \frac{n_s}{n} kT \sum_s \left[\frac{\partial n_s}{\partial t}\right]_{\substack{\text{coll} \\ \text{rad}}} , \qquad (77)$$

hence

$$\left(\frac{\partial n_s}{\partial t}\right)_T = \frac{n_s kT}{p} \sum_s \left[\frac{\partial n_s}{\partial t}\right]_{\substack{\text{coll.} \\ \text{rad.}}} . \qquad (78)$$

A temperature change at p = constant leads in addition to the following rate for n_s

$$\left(\frac{\partial n_s}{\partial t}\right)_p = - \frac{n_s}{T} \left(\frac{\partial T}{\partial t}\right)_p . \qquad (79)$$

Thus, for the species s the following rate equation is obtained

$$\frac{\partial n_s}{\partial t} = \left[\frac{\partial n_s}{\partial t}\right]_{\substack{\text{coll.}\\ \text{rad.}}} + \frac{n_s kT}{p}\sum_s \left[\frac{\partial n_s}{\partial t}\right]_{\substack{\text{coll.}\\ \text{rad.}}} - \frac{n_s}{T}\left(\frac{\partial T}{\partial t}\right)_p . \tag{80}$$

A coupled system of rate equations of type (80) has been applied by Brand and Kopainsky [70] in the frame of a simplified reaction model that takes the following chemical species into account :

$$F,\ F_2,\ S,\ S_2,\ SF,\ S^+,\ S_2^+,\ F^-\ \text{and electrons}\ .$$

Figure 13 shows the results of the model calculations. The initial condition is $T = 10^4$ K at $t = 0$, with the particle densities given by their equilibrium values at $p = 1$ atm. During the first 50 μs, there is a strong electron-S^+ ion recombination, the F^- density remains approximately constant. At 50 μs begins a drastical change of the neutral particle densities. For $t > 100$ μs, the ion density stabilizes at a value of approximately 10^{13} cm^{-3}. The most abundant ions are S_2^+ and F^-, the electron density is negligible for $t > 100$ μs. The formation of F^- and S_2^+ ion pairs leads to a longlived negative ion plasma which determines the electrical properties of the gas and, thus, a possible dielectric failure when the voltage reappears at the electrodes.

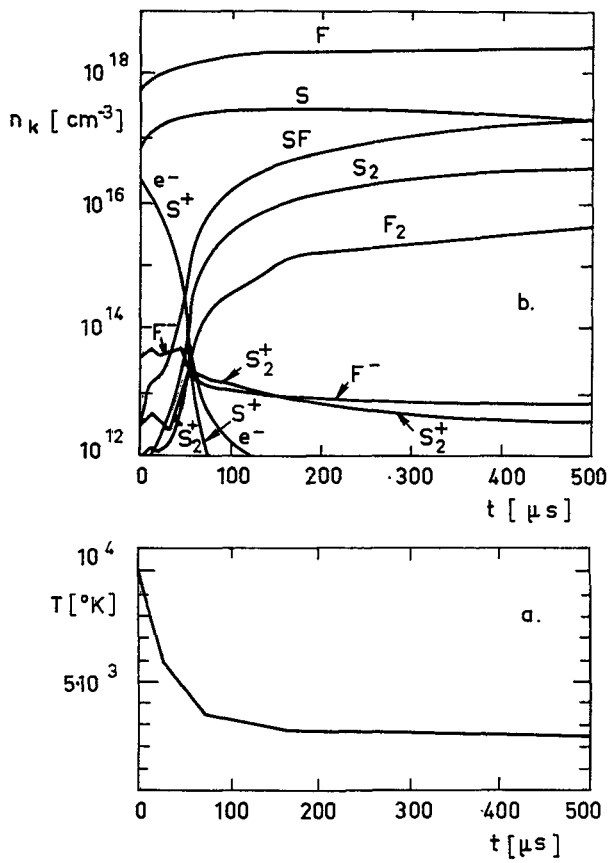

Fig. 13. — Temporal evolution of plasma composition (particle densities n_k of chemical species k) and temperature T of a recombining SF_6 plasma at a pressure of 1 atm, after [70].

5. **Collisional-radiative recombination.** — The eqs. eqs. (21*a*), (21*b*) permit to define two different collisional-radiative recombination (α) and ionisation coefficients (S) for the electrons and the ions :

$$\frac{\partial n_e}{\partial t} + \nabla_r\cdot(n_e \langle V_e \rangle) = n_e[n_0\, S_e - n_+\, \alpha_e] \tag{81a}$$

$$\frac{\partial n_+}{\partial t} + \nabla_r\cdot(n_+ \langle V_+ \rangle) = n_e[n_0\, S_+ - n_+\, \alpha_+] . \tag{81b}$$

For negative ions, a third equation has to be added. In negative ions-free plasmas,

$$S_e = S_+ = S\ , \qquad \alpha_e = \alpha_+ = \alpha\ ,$$

and eq. (22) hold.

The recombination coefficient α can be determined experimentally by measuring $n_e(r, t)$ of a recombining plasma at sufficiently low temperature (in order to avoid perturbation by the term $n_e\, n_0\, S$).

For *constant volume*, α is given by

$$\alpha = -\frac{1}{n_+\, n_e}\left[\frac{\partial n_e}{\partial t} - D_a \nabla^2 n_e\right] . \tag{82}$$

The decrease of the electron density is accompanied by a decrease of total pressure with a rate

$$\left(\frac{\partial p}{\partial t}\right)_V = kT\sum_s \left[\frac{\partial n_s}{\partial t}\right]_{\substack{\text{coll.}\\ \text{rad.}}} + nk\left(\frac{\partial T}{\partial t}\right)_V . \tag{83}$$

The last term accounts for a change of temperature during the recombination phase.

When the plasma recombines at *constant pressure* we can as a first approximation apply eq. (80) to which the ambipolar diffusion term should still be added. Putting in eq. (80) $n_s = n_e$ we obtain

$$[\partial n_s/\partial t]_{\substack{\text{coll.}\\ \text{rad.}}} = [\partial n_e/\partial t]_{\substack{\text{coll.}\\ \text{rad.}}} = -\, n_e\, n_+\, \alpha\ .$$

Further, $\sum_s [\partial n_s/\partial t]_{\substack{\text{coll.}\\ \text{rad.}}}$ is given by eq. (13). It thus follows

$$\alpha = -\frac{1}{n_e\, n_+(1 + n_e\, kT/p)}\left[\frac{\partial n_e}{\partial t} - D_a \nabla^2 n_e - \right.$$
$$\left. - \frac{n_e\, kT}{p}\left[\frac{\partial n_M}{\partial t}\right]_{\substack{\text{coll.}\\ \text{rad.}}} + \frac{n_e}{T}\left(\frac{\partial T}{\partial t}\right)_p\right] . \tag{84}$$

The third term — which is generally positive — accounts for the formation of neutral molecules during the recombination phase. In the denominator, the ratio of electron pressure to total pressure can in almost all cases be neglected. During recombination, T practically equals the gas temperature. When measurements of $n_e(r, t)$ and $T(t)$ are based on methods in which the length of the plasma column intervenes, corrections have eventually to be made in order to account for the contraction of the plasma column.

Substituting in eqs. (82) and (84) n_e by n_- yields the corresponding expressions for the recombination coefficient of a negative ion plasma in (which electrons are absent).

From figure 13 we can extract the order of magnitude of the recombination coefficient. One finds $\alpha \approx 10^{-8}$ cm^3 s^{-1} for the first 50 μs, and

$$\alpha \approx 10^{-10} \text{ cm}^3 \text{ s}^{-1}$$

for times $t > 100$ μs. These values differ by several orders of magnitude from those measured for the cold SF_6 gas [71] which contains mainly SF_5^+, SF_5^- and SF_6^- ions and probably also cluster ions of the form $SF_6^-(SF_6)_x$.

6. **Atomic processes in high-temperature plasmas.** — Until now, we have dealt with relatively cool plasmas containing both atomic and molecular (neutral and ionised) species. We will now consider high-temperature plasmas. We shall limit the discussion to a selected number of atomic (ionic) processes encountered in so-called thermonuclear fusion plasmas. In the following, the word *hydrogen* is employed for either of the isotopes hydrogen, deuterium and tritium. The examples chosen apply in the first place to Tokamak plasmas.

6.1 THE DYNAMICS OF HYDROGEN ATOMS. — Apart from laser-fusion experiments, all *fusion plasmas* are submitted to strong magnetic fields in order to confine the plasma and to separate it from material walls. However, only charged particles are influenced by a magnetic field, neutrals can cross it without being affected. Owing to ion-electron recombination, the neutral particle density is not zero, but even under thermonuclear conditions can some neutral hydrogen atoms be present in the hot plasma core. One has

$$n(H^0) \approx 10^6 \ldots 10^8 \text{ cm}^{-3} .$$

This follows directly from the solution of the ionisation-recombination balance for hydrogen and agrees approximately with measured values. Therefore, energetic ions $H^+(D^+, T^+)$ can undergo charge exchange collisions with neutral atoms $H^0(D^0, T^0)$ according to the reaction

$$\underline{H}^+ + H^0 \rightarrow \underline{H}^0 + H^+ \qquad (85)$$

in which the energetic ions $\underline{H}^+$ are transformed into energetic neutral particles $\underline{H}^0$ which can now cross the magnetic barrier. Whether these neutrals can directly reach the walls or not depends on the probability of re-ionisation, since a re-ionised particle will again be captured by the magnetic field. The ionisation probability depends on the ionisation cross-sections. In figure 14, all relevant ionisation cross-sections are compared with those for charge exchange. One sees that for kinetic energies $E \leqslant 60$ keV (that is for the whole region of thermo-nuclear interest), the charge exchange cross-sections are larger than the ionisation

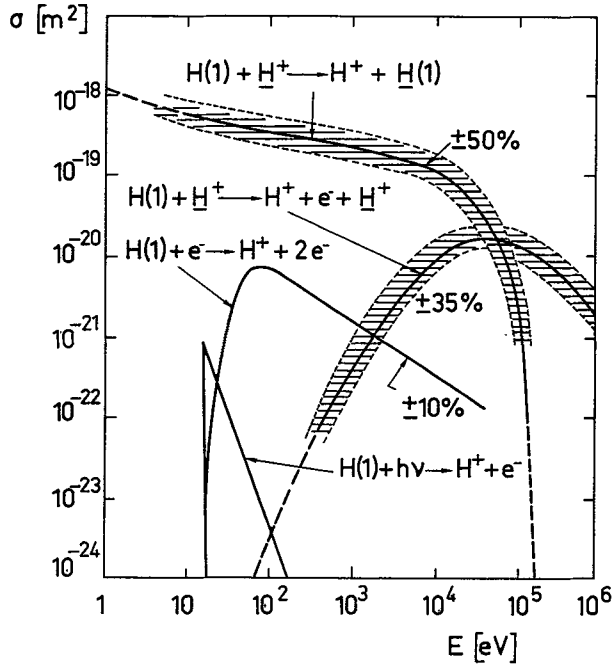

Fig. 14. — Cross-sections σ for charge exchange and ionisation of neutral hydrogen atoms (or their isotopes) in the ground state.

cross-sections. It follows from this that energetic neutral atoms can reach the walls where they cause sputtering of wall material [73, 74]. This represents a source of impurities.

Recent calculations [75] for the future Princeton Tokamak TFTR (now under construction) have led to the result that, due to charge exchange reactions, the flux of charge exchange neutrals will correspond to a total energy loss rate of 1 MW, that the *mean* kinetic energy of a neutral atom impinging on the wall will be 1.9 keV, and that sputtering of the stainless steel walls will result in a flux of $1.5 \cdot 10^{17}$ iron atoms/m^2 s. In one second, one will build-up a mean iron impurity concentration of approximately one percent. This can prevent thermonuclear ignition.

This example shows how important are technical solutions which minimize sputtering and avoid penetration of impurities into the plasmas. Possible solutions to this problem are the formation of cold-plasma blankets [76], mechanical divertors (scrape-off limiters) [77] or magnetic divertors [78] in connection with the development of materials having low sputtering yields.

6.2 THE DYNAMICS OF HELIUM. — The ideal fusion plasma should only contain D^+ and T^+ ions and electrons at temperatures of the order of 10^8 K $\triangleq$ 10 keV. In the absence of thermonuclear reactions, the only radiation processes would be electron-ion bremsstrahlung and cyclotron radiation. Both processes represent energy losses which must be compensated by some heating mechanism in order to avoid cooling of the plasma. In a continuously operated magnetically confined D − T fusion plasma (Tokamak plasma),

this heating mechanism will be provided by the thermonuclear reaction itself :

$$^2D + {}^3T \rightarrow {}^4He\ (3.5\ MeV) + {}^1n\ (14.1\ MeV)\,. \quad (86)$$

The He-ions (α particles) produced in the reaction are captured by the confining magnetic field. At $B = 4$ tesla their Larmor radius is 7 cm. The energetic α particles make collisions with the colder ion-electron gas and heat it up (so-called α-particle heating). This heating mechanism also compensates energy losses due to diffusion (charge exchange, heat conduction, ...).

The production of helium nuclei increases the ion charge state of the plasma and, thus, the bremsstrahlung losses. The plasma must therefore continuously increase its temperature in order to compensate the increasing radiation losses. The compensation is possible, since the power of the fusion reaction (86) increases exponentially with T whereas the rate of the bremsstrahlung losses increases only proportionally to $T^{1/2}$ (for the details, see e.g. [79-80].) The fusion reaction (86) leads to a kind of self-contamination. In order to avoid this effect and to keep the energy losses and temperature low, a rapid exhaust of the helium is desirable. The helium leaving the reactor is then replaced by new fuel. In a continuously operated reactor, the helium can only leave the hot reaction zone by diffusion. Both Coulomb- and atom-ion collisions can play a role.

The physical situation is shown in figure 15. Helium is assumed to be the only impurity element. He^{2+} will be produced in the plasma core. The exact radial distribution of He^{2+}, He^+ and He^0 will depend on various collective processes but also on individual atomic reactions. Let us consider first the He^{2+} ions.

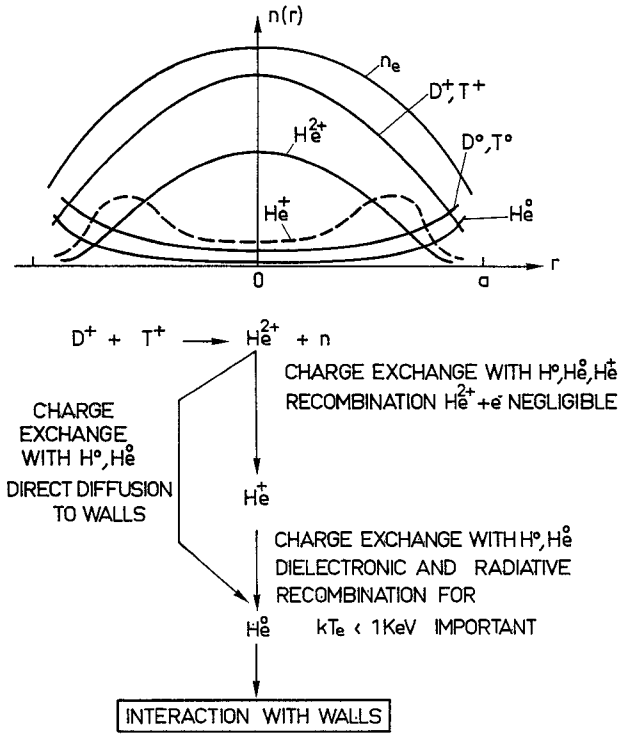

Fig. 15. — Radial distribution of helium in a hypothetical D-T fusion reactor, and possible elementary reactions which may have an influence on the exhaust of helium.

The He^{2+} ions can be transformed in He^+ and He^0 by different reactions. In a future reactors collisions with the neutral D^0 and T^0 atoms may become important. The density of the neutrals is not zero, but varies from approximately 10^8 cm^{-3} at the axis to 10^{10} cm^{-3} at the plasma boundary. Figure 16 shows the cross-sections for the non-symmetrical charge exchange between He^{2+} and H^0. The reaction

$$He^{2+} + H(1s) \rightarrow He^+(2s, 2p) + H^+ \quad (87)$$

has an accidental resonance leading to an especially large cross-section.

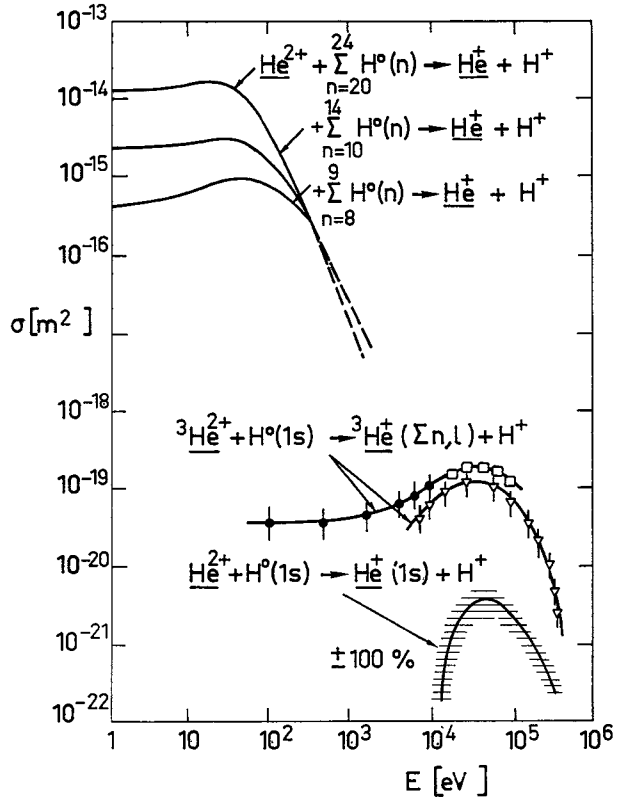

Fig. 16. — Charge exchange cross-sections for collisions between He^{2+} ions and neutral hydrogen atoms (which can be considered as representative for the isotopes D and T), after [82-84].

In a fusion plasma, there will be a relatively large number of excited D^0 and T^0 atoms (compared to those in the ground state). Owing to the extremely large charge exchange cross-sections for the excited levels, the excited particles can play a role in the transport of the helium ions. The change from He^{2+} to He^+ leads to an increase of the Larmor radius and, thus, contributes to the diffusion flux. The He^+ ions are still captured by the magnetic field.

The dynamics of the He^+ ions will now depend on whether back-ionisation into He^{2+} or further transformation into He^0 through charge exchange or

recombination occurs. Back-ionisation into He^{2+} will mainly occur through electron collisions. Figure 17 shows the relevant ionisation cross-sections.

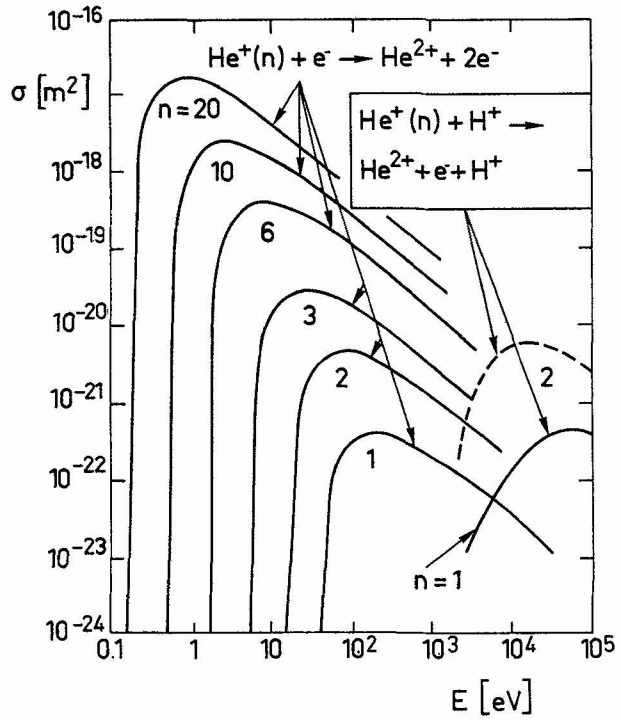

Fig. 17. — Cross-sections for ionisation of He^+ into He^{2+}, after [37], [83-85].

Also are shown the cross-sections for ionisation by proton impact. There do not exist any studies in which the relevant atomic collision processes have been taken into account. For further details concerning the exhaust problem, the reader is referred to [81].

6.3 THE DYNAMICS OF OXYGEN. — Special attention must be paid to oxygen which is found with relatively high concentration (0.5 % to 5 %) in nearly all Tokamak plasmas. The physical situation is schematically shown in figure 18. Neutral oxygen atoms diffuse from the walls into the plasma-wall boundary layer where they are ionised. An ionised oxygen atom is captured by the magnetic field. Further ionisation will lead to O^{2+} ions, etc. The ions will essentially diffuse due to Coulomb collisions and eventual collective effects. However, it is also possible that the ions undergo charge exchange collisions with neutral hydrogen atoms according to the reaction

$$\underline{O}^+ + H^0 \rightarrow \underline{O}^0 + H^+ . \qquad (88)$$

Thus, the neutral oxygen atom can again diffuse across the magnetic field. Figure 19 shows the relevant cross-sections intervening in the ionisation and charge exchange processes [82, 86]. One clearly sees that charge exchange can play a dominant role. A recent study [87] has shown that, due to the high charge exchange cross-section, up to 30 % of the oxygen atoms leaving the walls are reflected back to the walls. In this study, only the following three reactions were taken into account :

$$O^0 + e^- \rightarrow O^+ + e^- + e^- \qquad (89a)$$

$$O^+ + e^- \rightarrow O^{2+} + e^- + e^- \qquad (89b)$$

$$\underline{O}^+ + H^0 \rightarrow O^0 + H^+ . \qquad (89c)$$

It might be that also other chemical reactions such as :

$$O^+ + H_2^0 \rightleftarrows OH^+ + H^0 \qquad (90a)$$

$$OH^+ + e^- \rightleftarrows O^0 + H^0 \qquad (90b)$$

$$OH^0 + H^0 \rightleftarrows OH^0 + H^+ \qquad (90c)$$

$$O_2^+ + e^- \rightleftarrows 2\,O^0 + e^- \qquad (90d)$$

$$[H_3O]^+ + e^- \rightleftarrows [H_2O]^0 + H^0 \qquad (90e)$$

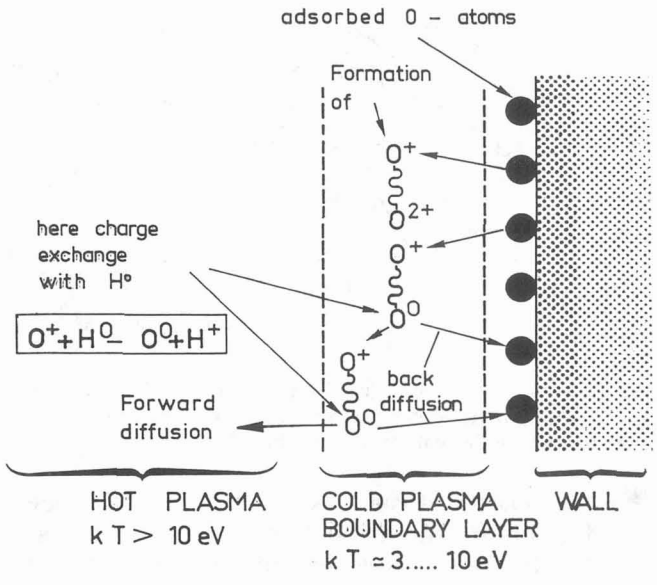

Fig. 18. — Diffusion of oxygen through a cold plasma boundary layer.

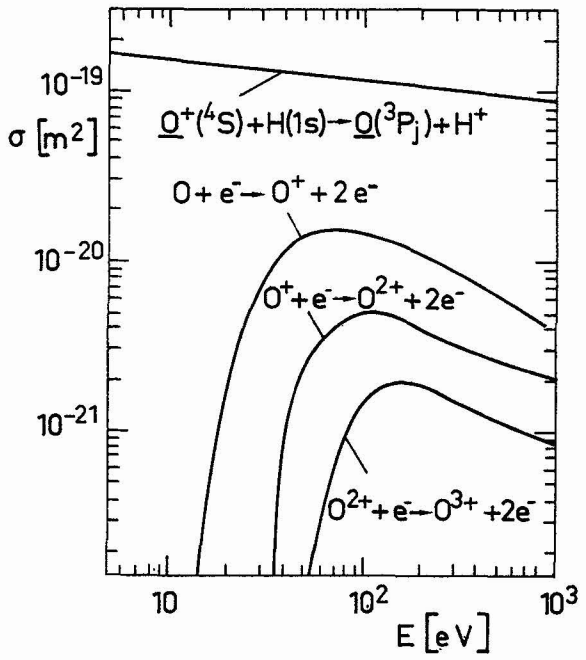

Fig. 19. — Cross-sections σ for oxygen, after [82, 85].

are of importance in the immediate vicinity of the walls. Corresponding studies are missing in the litterature.

6.4 RADIATION LOSSES. — High Z-impurities — even in very small concentrations — in thermonuclear fusion plasmas can lead to high radiation losses. This can have severe consequences for the global energy balance in future thermonuclear reactors. The same problem is met in present-day fusion research machines of the Tokamak type.

Figure 20 shows how the different physical processes contribute to the power loss of the Tokamak TFR-400 [90]. The mean radius of the torus is $R = 98$ cm, the outer plasma radius is $r = 20$ cm, r being the distance from the center of the plasma. The figure shows the power which is deposited in a plasma volume defined by the value of r and the power which is lost through the surface surrounding the plasma at r. In the case of figure 20*a*, the plasma is only heated by the electric current circulating in the plasma (ohmic heating). The power density is $\dot{\Omega}$, see eq. (19). In the case of figure 20*b*, the plasma is additionally heated by an energetic neutral particle beam with power density $\dot{I}$. In the first case, the total power input is 570 kW, in the second case 870 kW. One sees that approximately 50 % of the total energy are lost in form of radiation. The latter contributes especially in the outer zones to the energy loss.

In a pure completely ionised hydrogen (D – T) plasma the only radiation loss originates from free-free bremsstrahlung radiation and cyclotron radiation. But already small admixtures of heavy species increase the radiation loss considerably : as long as the atomes are not completely stripped, electronic excitation will cause intense bound-bound radiation; also electron-ion recombination will partly be responsible for this enhanced radiation loss (free-bound and dielectronic recombination radiation), see eq. (20). The contribution of the free-free radiation of not completely stripped atoms is small. However, for completely ionised particles the power density of the bremsstrahlung caused by impurities can dominate the radiation loss of a plasma completely.

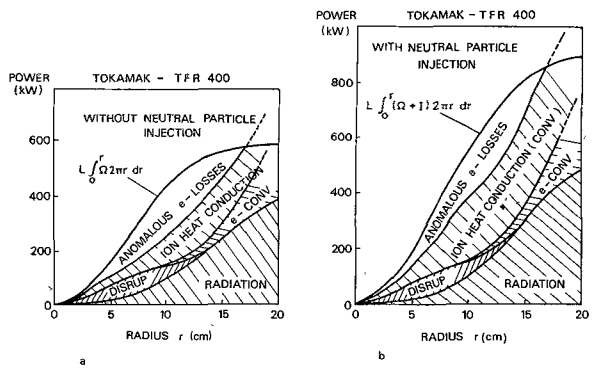

Fig. 20. — Power input into the french Tokamak TFR-400 as a function of radius, and contribution of the various processes to the power loss, after [90]. *a*) only ohmic heating, *b*) ohmic heating plus neutral particle injection heating.

The radiation losses caused by impurities in Tokamaks are generally calculated in the frame of the corona model, because of the very high electron temperatures and relatively low electron densities. Figure 21 gives an example for molybdenum which has been used in Tokamaks as current-limiting diaphragme. The individuel contributions to the total power loss have been typified in eq. (20). Similar calculations have been carried out in different laboratories for many other impurity species and the data are available in the literature. In more sophisticated model calculations also spatial relaxation effects due to diffusion are taken into account [92]. The application of the *corona model* — with superposed diffusion fluxes of the ground state ions — gives satisfactory results for the global radiative loss rates. However, the application of this model to the calculation of the intensity of special spectral lines may in some cases lead to erroneous results, due to strong collisional coupling between various levels compared to radiative coupling by spontaneous de-excitation. If such spectral lines are used for diagnostic purposes, their intensities should be calculated in the frame of a more general collisional-radiative model in which all important reactions are taken into account. Especially charge exchange reactions into excited levels should be taken into account. For further details see e.g. the review [88].

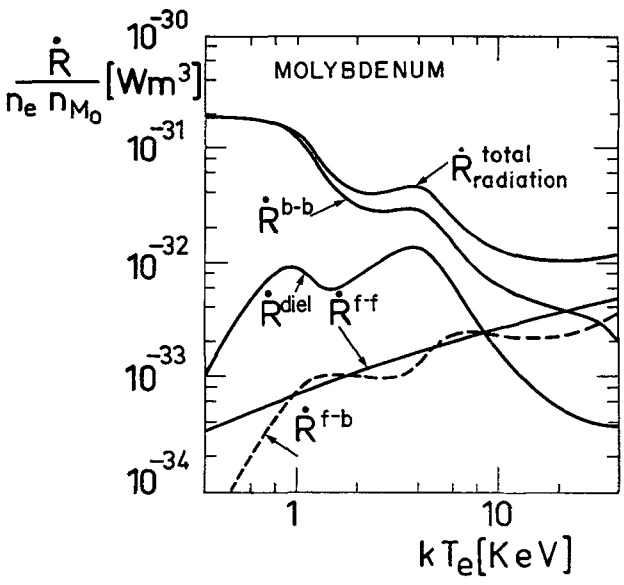

Fig. 21. — Radiation loss rate for molybdenum. $\dot{R}/n_e n_{Mo}$ is the power density radiated per electron and per molybdenum particle, after [91]. The individual contribution have been defined in eq. (20).

7. **Summary and conclusion.** — In order to understand the physical (and also the chemical) properties of non-L.T.E. plasmas one has to study in detail the coupled system of collisional-radiative equations for the particle densities, momenta and energies. Owing

to the complexity of the problem in general, and due to the sometimes scarce knowledge of the reaction processes in particular, many simplifying assumptions have often to be made. In this paper, three different types of non L.T.E. plasmas have been treated : glow discharge, negative ion and Tokamak plasmas. The discussion has been restricted to stationary and quasi-stationary states and to laser-induced fluorescence. In selected examples it has been shown how the application of the rate equations permits to interprete and to calculate special plasma properties on the one hand, and how the rate equations allow to extract information about special, dominant collision processes and to determine their rate coefficients on the other hand. In principle, quite similar problems are encountered in all other types of non-L.T.E. plasmas, fast transient plasmas included with the additional difficulty, however, that the time-dependent coupling may require the treatment of a (much) larger number of coupled rate equations compared to the stationary and quasi-stationary states. — The processes which are taken into account in the rate equations should satisfy the condition of micro-reversibility. When this condition is not fulfilled, the rate equations lead to inconsistent results from the thermodynamic point of view.

References

[1] EBELING, W., KRAEFT, W. D., KREMP, D., Theory of Bound States and Ionization Equilibrium in Plasmas and Solids, in *Ergebnisse der Plasmaphysik und der Gaselektronik*, Bd. 5 (Ed. R. Rompe and M. Steenbeck), Akademie Verlag, Berlin, 1976.

[2] KRAEFT, W. D., Non-ideal Plasmas, Elementary Excitations and Macroscopic Properties, in *The Physics of Ionized Gases* (Ed. R. K. Janev), The Institute of Physics, Beograd, 1978.

[3] POPOVIČ, M. M., Measured Properties of Non-ideal Plasmas, in *The Physics of Ionized Gases* (Ed. R. K. Janev), The Institute of Physics, Beograd, 1978.

[4] BURGESS, D. D., Spectroscopic Effects in Dense and Ultra-dense Plasmas, in *The Physics of Ionized Gases* (Ed. R. K. Janev), The Institute of Physics, Beograd, 1978.

[5] FRANCIS, G., The Glow Discharge at Low Pressures, in *Handbuch der Physik*, vol. XXII (Ed. S. Flügge), Springer Verlag, 1956, p. 53-208.

[6] VON ENGEL, A., Ionization in Gases by Electrons in Electric Fields, in *Handbuch der Physik*, vol. XXI (Ed. S. Flügge), Springer Verlag, 1956, p. 504-573.

[7] VON ENGEL, A., *Ionized Gases*, Clarendon Press, Oxford, 2nd ed., 1965, p. 238-248.

[8] DELCROIX, J. L., *Physique des Plasmas*, tome 2, Dunod Editeur, Paris, 1966.

[9] DRAWIN, H. W., Transport Properties of Plasmas, in *Reactions under Plasma Conditions*, vol. 1 (Ed. M. Venugopalan, Wiley-Interscience), New York, 1971.

[10] HIRSCHFELDER, J. O., CURTIS, Ch. F., BIRD, R. B., *Molecular Theory of Gases and Liquids*, John Wiley and Sons, 1954.

[11] FINKELNBURG, W., MAECKER, H., Elektrische Bögen und Thermisches Plasma, in *Handbuch der Physik*, vol. XXII (Ed. S. Flügge), Springer Verlag, 1956, p. 254-444.

[12] HEADRICK, L. B., DUFFENDACK, O. S., *Phys. Rev.* **3A** (1931) 736.

[13] DOTE, T., KANEDA, T., *Phys. Letts.* **48A** (1974) 351.

[14] WILHELM, H. E., *J. Math. Phys.* **13** (1972) 252.

[15] WILHELM, H. E., LIRON, N., *Phys. Fluids* **15** (1972) 1328.

[16] WILHELM, H. E., *Canad. J. Phys.* **50** (1972) 1156.

[17] DRAWIN, H. W., EMARD, F., KATSONIS, K., *Z. Naturforsch* **28a** (1973) 1422.

[18] DRAWIN, H. W., EMARD, F., DUBREUIL, B., CHAPELLE, J., *Beitrage aus der Plasmaphysik* **14** (1974) 103.

[19] DUBREUIL, B., CATHERINOT, A., *J. de Physique* **39** (1978) 1071.

[20] LEWIS, J. W., WILLIAMS, W. D., *J. Quant. Spectr. Radiative Transfer* **16** (1976) 939.

[21] CAPITELLI, M., DILONARDO, M., MOLINARI, E., *Chem. Physics* **20** (1977) 417.

[22] CACCIATORE, M., CAPITELLI, M., DILONARDO, M., *Chem. Physics* **34** (1978) 193.

[23] CAPEZZUTO, P., CRAMAROSSA, F., D'AGOSTINO, R., MOLINARI, E., *J. Phys. Chem.* **79** (1975) 1487 ; **80** (1976) 882.

[24] POLAK, L. S., SERGEEV, P. A., SLOVETSKII, D. I., *High Temperature* **15** (1977) 13.

[25] CAPITELLI, M., DILONARDO, M., *Rev. de Physique Appl.* **13** (1978) 115.

[26] WINKLER, R., PEAU, S., *Beitrage aus der Plasmaphysik* **13** (1973) 273 ; **14** (1974) 167.

[27] PFAU, S., WINKLER, R., *Beitrage aus der Plasmaphysik* **18** (1978) 113.

[28] ENGELKE, B.-E., *Z. Physik* **158** (1960) 422.

[29] PFAU, S., RUTSCHER, A., *Beiträge aus der Plasmaphysik* **8** (1968) 73.

[30] WOJACZEK, K., *Beiträge aus der Plasmaphysik* **6** (1966) 211.

[31] ALBRECHT, G., ECKER, G., MÜLLER, K. G., *Z. Naturforsch.* **17a** (1962) 854.

[32] WOJACZEK, K., *Beiträge aus der Plasmaphysik* **7** (1967) 149.

[33] WOJACZEK, K., *Beiträge aus der Plasmaphysik* **8** (1968) 109.

[34] WOJACZEK, K., *Beiträge aus der Plasmaphysik* **9** (1969) 243.

[35] SMITS, R. M. M., PRINS, M., *Physica* **96C** (1979) 243.

[36] SMITS, R. M. M., PRINS, M., *Physica* **96C** (1979) 262.

[37] MASSEY, H. S. W., GILBODY, H. B., *Electronic and Ionic Impact Phenomena*, vol. 4, Clarendon Press, Oxford, 1974.

[38] LORENTS, D. C., The Physics of Electron Beam Excited Rare Gases at High Densities, in *Proc. 11th Intern. Cong. on Phenomena in Ionized Gases*, Eindhoven, 1975, part 2, invited papers (Eds. J. G. A. Hölscher and D. C. Schram), North Holland, Amsterdam, 1976. See also *Physica* **82C** (1976) 19.

[39] NEIGER, M., *Z. Naturforsch.* **30a** (1975) 474.

[40] POPP, H.-P., *Vacuum* **24** (1974) 551.

[41] POPP, H.-P., KRUSE, S., *J. Quant. Spectr. Radiat. Transfer* **16** (1976) 683.

[42] BEHRINGER, K., THOMA, P., *Physical Rev.* **17** (1978) 1408.

[43] HOFFMANN, H., *J. Quant. Spectr. Radiat. Transfer* **21** (1979) 163.

[44] D'YACHKOV, L. G., KOBZEV, G. A., *High Temperature* **14** (1976) 607.

[45] RISLEY, J. S., EDWARDS, A. K., GEBALLE, R., *Phys. Rev. A* **9** (1974) 1115.

[46] RISLEY, J. S., DE HEER, F. J., KERKDIJK, C. B., *J. Phys. B* (Atom. Molec. Phys.) **11** (1978) 1783.

[47] WILLIAMS, F., WILLIS, B. A., *J. Phys. B* (Atom. and Molecular Physics) **7** (1974) L61.

[48] BEHRINGER, K., THOMA, P., *Phys. Rev. A* **17** (1978) 1408.

[49] MACEK, J. H., BURKE, P. G., *Proc. Phys. Soc.* **92** (1967) 351.

[50] BROAD, J. T., REINHARDT, W. P., *Phys. Rev. A* **14** (1976) 2159.

[51] SCHMELTEKOPF, A. L., FEHSENFELD, F. C., FERGUSON, E. E., *Astrophys. J.* (Letters) **148** (1967) L155.

[52] SCHMELTEKOPF, A. L., FELSENFELD, F. C., FERGUSON, E. E., *Astrophys. J.* (Letters) **148** (1967) L155.

[53] BIENIEK, R. J., DALGARNO, A., *Astrophys. J.* **228** (1979) 635.

[54] NICOLOPOULOU, E., BACAL, M., DOUCET, H. J., *J. de Physique* **38** (1977) 1399.

[55] BACAL, M., HAMILTON, G. W., *Phys. Rev. Letts.* **42** (1979) 1538

[56] BACAL, M., HAMILTON, G. W., BRUNETEAU, A. M., TAILLET, J., *Rev. Sci. Instr.* **50** (1979) 719.

[57] HISKES, J. R., BACAL, M., HAMILTON, G. W., *Atomic Reactions in H^- and D^- Plasmas*, Report UCID-18031, Lawrence Livermore Laboratory, 1979.

[58] FRIE, W., *Z. Physik* **201** (1967) 269.

[59] LIEBERMANN, R. W., LOWKE, J. J., *J. Quant. Spectros. Radiat. Transfer* **16** (1976) 253.

[60] RAGALLER, K., Physics of Arcs in Circuit Breakers, p. 251-268, in *Proc. (invited lectures) 13th Intern. Conf. on Phenomena in Ionized Gases*, September 12-17, 1977, Berlin; Editor Physical Society of the German Democratic Republic, 1977.

[61] JACOB, T., SCHADE, E., SCHAUMANN, R., *Self-blasting, a new switching principle for economical SF_6 Circuit Breakers*. C.I.R.E.D., London 1977, I.E.E. Conf. paper No. 2.4, p. 63-66.

[62] BRINKHOFF, R., BECKER, H., HÖGG, H., SCHMIDT, K. D., SCHMIDT, W., SONDEREGGER, G., Auslegung und Prüfung der metallgekapselten SF_6-isolierten 420 kV-Schaltanlage Frankfurt/Südwest; *Elektrizitätswirtschaft* **2** (1977) 21.

[63] KRENICKY, A., SCHADE, E., Recent Investigations on Arcs in SF_6 Gas-blast Breakers and Application of the Results to the Development of H.-V. Switchgear, paper No. 74, Section 2, *World Electrotechnical Congress*, June 21-25. Moscow, 1977.

[64] HERTZ, W., MENTEL, J., TIEMANN, W., *Siemens Forsch. und Entwickl. Ber.* **3** (1974) 5.

[65] HERTZ, W., MENTEL, J., STROH, J., TIEMANN, W., *Siemens Forsch. und Entwickl. Ber.* **4** (1975) 281.

[66] HERMAN, W., RAGALLER, K., IEEE Transact. on Power Apparatus and Systems, *PAS*-**96** (1977) 1546.

[67] HERMAN, W., KOGELSCHATZ, V., NIEMEYER, L., RAGALLER, K., SCHADE, E., IEEE Transact. on Power Apparatus and Systems, *PAS*-**95** (1976) 1165.

[68] RAGALLER, K., REICHERT, K., in *Current Interruption in High-Voltage Network* (K. Ragaller, ed.,), Plenum Press, New York 1978, p. 1-28.

[69] KOPAINSKY, J., in *Current Interruption in High-Voltage Networks* (K. Ragaller, ed.), Plenum Press, New York 1978, p. 329-354.

[70] BRAND, K. P., KOPAINSKY, J., *Appl. Phys.* **16** (1978) 425.

[71] SCHMIDT, W. F., JUNGBLUT, H., *J. Phys. D* (Appl. Phys.) **12** (1979) L 67.

[72] DRAWIN, H. W., EMARD, F., *Physica* **94C** (1978) 134.

[73] VERNICKEL, H., *Kerntechnik* **19** (1977) 279.

[74] TELLER, E., Peaceful Uses of Fusion, in *Proc. Second United Nations Int. Conf. on Peaceful Use of Atomic Energy*, Geneva, Sept. 1958, printed by The United Nations, Geneva, 1958, p. 27-33.

[75] GALLIGAN, J. G., GRALNIK, S. L., PRICE, W. G., Jr., KAMMASH, T., *Nuclear Fusion* **18** (1978) 63.

[76] ENGELMANN, F., GOEDHER, W. J., NOCENTINI, A., SCHÜLLER, F. C., Plasmas with Cold Blankets, in *Proc. Int. Symp. on Plasma-wall Interaction*, 18-22 Oct. 1976, Jülich, Editor : Kernforschungsanlage Jülich, Pergamon Press, Oxford 1977, p. 627-646.

[77] BIEGER, W., DIPPEL, K. H., FUCHS, G., WOLF, H., On Mechanical Divertors (Scrape-off Limiters), in *Proc. Int Symp. on Plasma-Wall Interaction*, 18-22 Oct. 1976, Editor Kernforschungsanlage Jülich, Pergamon Press, Oxford 1977, p. 609-618.

[78] KEILHACKER, M., Magnetic Divertors, in *Proc. Int Symp on Tokamak Reactors for Breakeven*, 21 Sept.-1 Oct. 1976, Erice (Ed. H. Knoepfel), Pergamon Press, Oxford 1977, p. 171-197.

[79] DRAWIN, H. W., *J. de Physique, Colloque C1* **40** (1979) 73-90.

[80] DRAWIN, H. W., *Atomkernenergie* **33** (1979) 182.

[81] HARBOUR, P. J., HARRISON, M. F. A., *Nuclear Fusion* **19** (1979) 695.

[82] FITE, W. L., SMITH, A. C. H., STEBBING, R. F., *Proc. Roy. Soc.* (London) **268** (1962) 527.

[83] SHAH, M. B., GILDOBY, H. B., *J. Phys. B* (Atom. and Molecul. Phys.) **11** (1978) 121.

[84] BURNIAUX, M., BROUILLARD, F., JOGNAUX, A., GOVERS, T. R., SZUCS, S., *J. Phys. B* (Atom. and Molecul. Phys.) **10** (1971) 2421.

[85] DRAWIN, H. W., *Z. Physik* **164** (1961) 513; Report EUR-CEA-FC-383, Fontenay-aux-Roses, 1966/67.

[86] HAMDAN, M., BIRKINSHAW, K., HASTED, J. B., *J. Phys. B* (Atom. and Molecul. Physics) **11** (1978) 331.

[87] COHEN, S. A., DYLLA, H. F., *Nuclear Fusion* **18** (1978) 5.

[88] DRAWIN, H. W., *Physics Reports* **37** (1978) 125-163.

[89] DRAWIN, H. W., Atomic and Molecular Structure and Collision Data with Application to Fusion Research, in *The Physics of Ionized Gases* (R. K. Janev, ed.). The Institute of Physics, Beograd, 1978.

[90] Equipe TRF, *Nuclear Fusion* **18** (1978) 1271.

[91] BRETON, C., DE MICHELIS, C., MATTIOLI, M., *J. Quantitative Spectrosc. Radiative Transfer* **19** (1978) 367.

[92] BOUJOT, J. P., MERCIER, C., WERKOFF, F., Report CISI-EUR-CEA, Makokot code d'évolution, Fontenay-aux-Roses, 1977.